CHALMERS

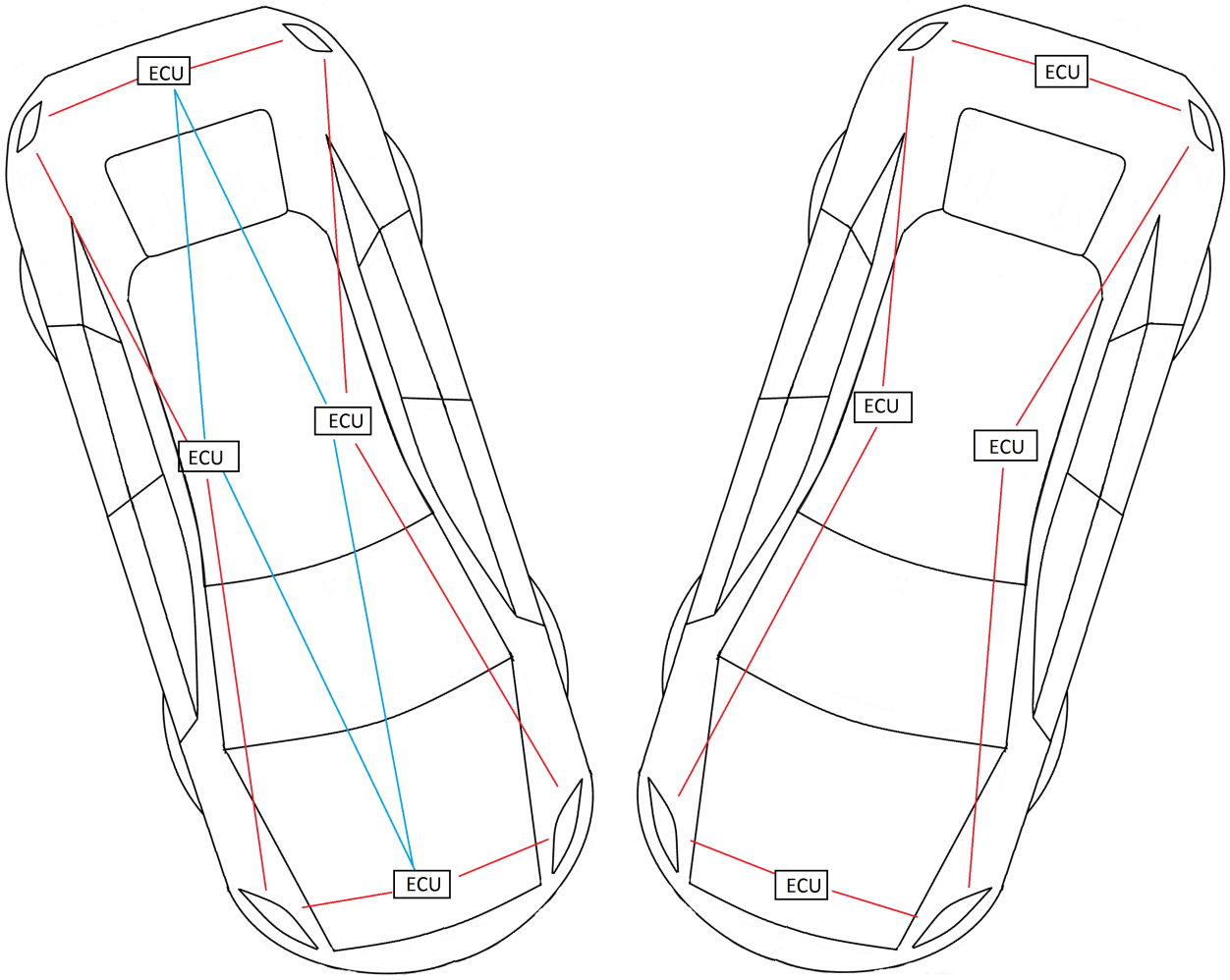

Vehicular Power-Line Communication Constraints

Master of Science Thesis in Embedded Electronic System Design

DANIEL JOSEFSSON
LENIN LAWRENCE

Department of Computer Science and Engineering
Chalmers University of Technology
Gothenburg, Sweden, August 2015

Vehicular Power-Line Communication Constraints
Daniel Josefsson, Lenin Lawrence

Examiner: Per Larsson-Edefors

Chalmers University of Technology
Department of Computer Science and Engineering
SE-412 96 Gothenburg
Sweden
Telephone +46 (0)31-772 1000

Cover image: Illustration of two vehicles with and without power-line communications. The vehicle to the left contains a separate data path (blue lines) for data transmission while the right vehicle with PLC has no separate data lines.

Department of Computer Science and Engineering
Gothenburg, Sweden, August 2015

Abstract

The increase of sensors and actuators in today's vehicles has led to a growing number of electronic control units (ECU). This increases the wiring harness of the vehicle, resulting not only in increased weight but also high installation and maintenance costs. This is mainly because the ECUs use protocols such as controller area network (CAN), local interconnect network (LIN), Flexray etc to communicate with each other. In this project, we conduct a feasibility study of power-line communication (PLC) using fixed point digital signal processors (DSP) in modern vehicles. The study focuses upon issues related to the transmission channel as well as the hardware. The issues related to the channel are addressed by proposing a model which includes the wiring harness and noise source. The hardware issues are addressed by implementing a signal chain consisting of a modulator and a demodulator using a fixed point DSP. Finally, the study shows that the processing hardware and the background noise does not prevent PLC from being a workable solution, instead it is the variation of the loads connected to the wiring harness that inhibits transmission over the power grid.

Keywords: Power-line Communication, Fixed Point Processor, Channel Modeling.

Acknowledgements

We would like to express our sincere gratitude to Dr. Lena Peterson, our supervisor at Chalmers University of Technology for providing valuable guidance and motivation throughout the project. Also we would like to thank Mr. Alixander Ansari and Mr. Andreas Eriksson, our supervisors from Sigma Technology for providing all the support and technical details of great importance.

We would like to especially thank Dr. Lars Svensson for the giving us insight regarding data collection, as well as E-sektionens Teletekniska Avdelning for providing their equipment during the project.

Daniel Josefsson and Lenin Lawrence, Gothenburg, August 2015

Contents

Acronyms

AC Alternating Current

ADC Analog-to-Digital Converter

AR Auto-Regressive

ARMA Autoregressive-Moving-Average

ARX AutoRegressive with eXternal input

AWG American Wire Gauge

BPSK Binary Phase Shift Keying

CAN Controller Area Network

CCS Code Composer Studio

DAC Digital-to-Analog Converter

DC Direct Current

DSP Digital Signal Processor

DTFT Discrete-Time Fourier Transform

ECU Electronic Control Unit

EMI Electromagnetic Interference

IDE Integrated Development Environment

LIN Local Interconnect Network

LTI Linear Time-Invariant

MCM Multi-Carrier Modulation

MOST Media Oriented Systems Support

OFDM Orthogonal Frequency Division Multiplexing

OSI Open System Interconnection

PLC Power-Line Communication

QAM Quadrature Amplitude Modulation

QPSK Quadrature Phase-Shift Keying

RRC Root Raised Cosine

SNR Signal to Noise ratio

SPI Serial Peripheral Interface

TI Texas Instruments

USB Universal Serial Bus

1

Introduction

The complexity of communication systems in modern vehicles has increased tremendously over the past decade in order to connect multiple electronic systems and sensor networks. Today's vehicles contain large number of circuits and sensors — in the range of 80 - 120 electronic control units (ECU). This demands an effective and reliable communication between the ECUs and other components [1].

Different protocols are used for establishing an effective communication between ECUs depending on quality-of-service (QOS) and bandwidth requirements. Both QOS and bandwidth requirements depend on the type of data being transferred between the ECUs, for example control data, safety data or infotainment data etc. According to Tuohy et al [2], some of the popular protocols used currently in the automobile industry are controller area network (CAN), Flexray, local interconnect network (LIN), media oriented system support (MOST) and belong to physical and data-link layers of open systems interconnection (OSI) network model (shown in Figure 2.3). In order to increase the bandwidth while maintaining reasonable QOS, the physical layer specification itself has to be changed as transmission characteristics of the medium act as constraints. For example in case of CAN the maximum data rate that can be transferred is 1Mbps and in case of Flexray it is 10Mbps, if the bandwidth is increased beyond the given constraints then signal reflections with high amplitude might increase jitter thereby inhibiting signal transmission [3].

According to Navet et al. [4], the significant increase in the number of ECUs has lead to complex architectures due to gateways between several clusters of both the same and/or different networking technologies. Gateways between clusters of similar networking technologies (CAN-CAN) include connections between buses with different priorities [5], for example refer Table 1.1.

Table 1.1: *CAN-CAN connections used at different priority levels.*

High priority	Bus connecting gearbox management system, engine management system, brake management system.
Medium priority	Bus connecting air processing system, instrument cluster system, locking and alarm system.
Low priority	Bus connecting automatic climate control system, clock and timer system, road transport information system.

Clusters of different technology include Flexray bus (acting as a backbone) connected to MOST, CAN and gateways between CAN and LIN. None of these protocols reduce the

number of cables, due to their topology rather the network still needs the same number of cables regardless of the speed and transmission quality. Therefore, the complexity of the wiring harness increases significantly due to the increase in connection points (usually more than 200) with several kilometres of cables. This situation not only creates a negative impact on the vehicle in terms of installation cost and mass (up to 50 kg) but also in terms of diagnostic and maintenance issues [6].

These disadvantages can be overcome by using power-line communication (PLC) technology. In PLC, data is transmitted over the direct current (DC) power grid of the vehicle, significantly reducing the number of cables, giving a clear advantage in terms of weight, space and cost [6]. Using PLC can establish a full-duplex mode of communication between different sets of components with the help of multi-carrier modulation (MCM) techniques. MCM is a technique in which the encoded/modulated (baseband) signal is transmitted on different carrier frequencies (passband) by employing frequency-division multiplexing [7].

With PLC, all devices connected to the power grid can communicate with each other simultaneously at different carrier frequencies with MC modulation techniques [8]. PLC can be implemented using either analog or digital modulation schemes, where digital modulation schemes have advantages over analog counterparts in terms of scalability and flexibility. However, digital modulation schemes require high-performance hardware which tends to be expensive. One of the ways to limit the hardware complexity and cost is to use fixed-point digital signal processors (DSP).

1.1 Background

As mentioned before, PLC is a technique in which data is transferred via the power grid. While PLC is an interesting option for some networks, it may not be suitable for safety-critical networks with strict reliability and standardization demands. However, PLC has been tested and evaluated for non-safety critical parts of the vehicle [9] and if PLC technology proves to be superior to existing networking techniques, a transition in all units connected to the network may be possible.

According to D'Orazio et al. [6], PLC's significant improvement in the residential market will make in-vehicle applications possible in the near future. However, existing PLC technology cannot be used directly due to the differences between the domestic power lines and vehicle's DC grid in terms of wire architectures, channel transfer function, ambient noise and grounding. In vehicles all electrical components use the chassis as ground, while in residential networks the nodes are instead connected with two wires to create an explicit return path for the current. The differences in grounding can be a source of electromagnetic compatibility and noise problems [10]. Additionally, using chassis as ground poses a problem due to the return path of the current since it chooses the path of least impedance, which varies depending on the loads connected to the wiring harness.

Efficient and reliable communication requires several challenges to be overcome; these include frequency selectivity of the channel caused by impedance mismatches in the wiring harness, as well as impulsive noise introduced by electrical components connected to it [11]. Needless to say, the major issue regarding PLC is the noise level in the channel.

Also, the state of the engine changes the noise characteristics of the channel which needs to be considered while designing a system [12]. Several studies have been performed regarding channel characterisation and variation of data rate at different points in the power grid using different modulation schemes and for different frequencies [13], [12], [8], the major findings are summarised below.

Noise present in the transmission channel can be broadly classified into two types: impulsive noise and background noise, among which the impulsive noise is more critical since it can reach an amplitude up to 100 V (characteristic values are between 0.5 V to 20 V). The impulsive noise is generated during the injection phase of the spark, produced by the spark plug of each cylinder inside the internal combustion engine which is one of the main sources of impulsive noise. Impulsive noise also occurs due to switching operations, either by the electrical components internally while driving or by passenger activities, hence it is highly random in nature. However, the impulsive noise can be modelled as a Poisson distribution since it is sporadic by nature. Additionally the background noise can be modelled by a Gaussian distribution [13].

Another major concern related to in-vehicle PLC is the frequency selectivity of the transmission channel due to multipath propagation, caused by impedance mismatches in the wiring harness [12]. According to Lienard et al. [14], it is not possible to obtain a precise configuration of the wiring harness in different vehicles due to the presence of several unknown impedances that vary over time. Furthermore, the input impedance of the wiring harness depends not only on the signal frequency but also on several other factors, such as the loads connected to the power grid and the loads connected to other cables from various electrical and/or electronic equipment.

According to Antoniali et al. [8], signal reflections, which are generated as a result of impedance mismatches, make the power grid an unfriendly media for communications. Therefore, a suitable modulation scheme is required to overcome the attenuation and frequency selectivity of the transmission channel, but such a modulation scheme leads to severe inter-symbol interference.

1.2 Aim

The aim of the project was to conduct a feasibility study of PLC using fixed point DSPs in modern vehicles. The study is conducted considering the issues related to the transmission channel as well as the hardware. The issues related to the channel are addressed by proposing a model for the channel which includes the wiring harness and the noise source. The hardware issues are addressed by implementing a signal chain using a fixed-point DSP consisting of a modulator and demodulator for basic modulation schemes.

1.3 Limitations

An off-line modelling approach has been used to estimate the channel model, that is, the model estimation is not performed based on data collected from the system continuously. Rather, the data was acquired by performing different experiments under various

conditions and subsequently used for modelling. Hence, the channel model is a mere approximation of the real system. Additionally, the data used for modelling the noise is from a single vehicle(truck) which makes the model specific for the vehicle.

1.4 Outline

The theoretical aspects required for the project are explained in Chapter 2. In Chapter 3 the basic setup used for acquiring data and a brief description of the methods approached is presented. The report is structured in a way that both channel model (Chapter 4) and hardware issues (Chapter 5) are described separately. In Chapter 6, both the issues are discussed together which is followed by conclusions at the end (Chapter 7).

2

Technical Background

The concept of transferring information over the power grid has been around since the 1900s and when regulations were introduced on the radio frequencies during World War II, experimentation on PLC by radio amateurs began. However, it was not until in the middle of the 1990s that the pace of research increased within the field. The main focus has been on supply system low-voltage power distribution networks within buildings and structures, for example local area networks is one application that has came up in recent years, illustrated in Figure 2.1. Additional research has been made on the usage of power grid for phone communication, which is of special interest in developing countries where construction of separate transmission lines is too costly [15].

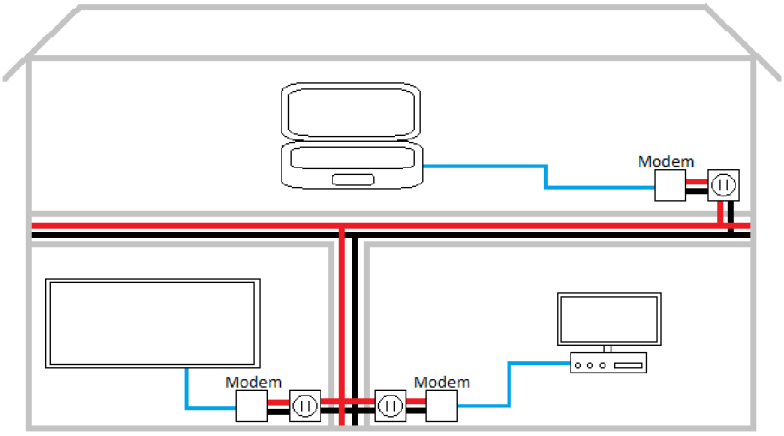

Figure 2.1: *Concept of residential power-line communication used for a local area network*

In contrast to the historically main focus when it comes to PLC, this project instead focuses on using PLC for vehicles. The major difference between residential PLC and its vehicular counterpart is the wiring topology. Wire sizes and loads in vehicles are largely different to those in a residential building [16], rendering the implementation significantly more complex as well. Since the power grid in a vehicle is not designed with communication in mind it is a hostile environment to transfer data over. Also, the cable attenuation at frequencies of interest is usually large [15].

The main purpose of implementing PLC in vehicles is to reduce the number of cables that will be used. Figure 2.2 displays the concept of how the ECUs connect only to the power grid instead of also being connected to the CAN bus as in most current vehicles.

Such a setup will reduce both weight, space and cost of installation.

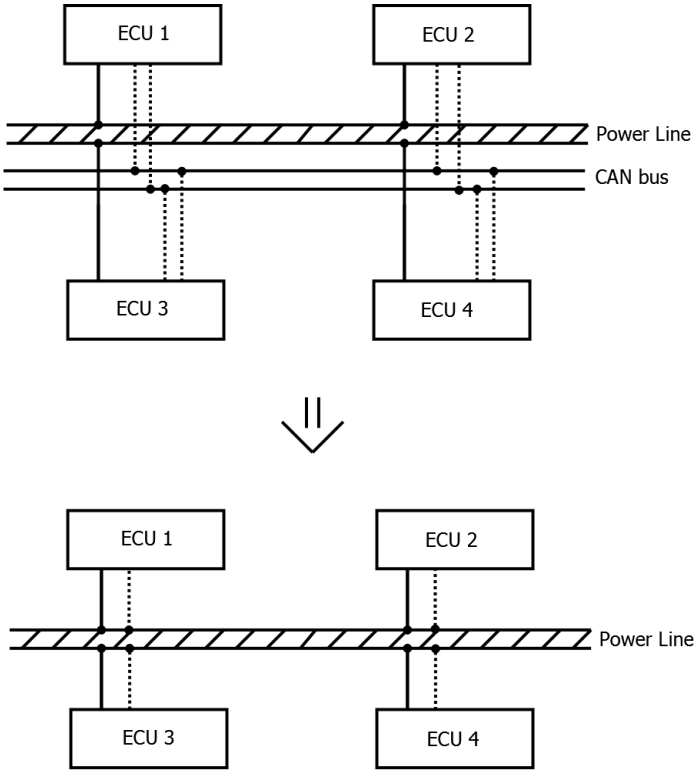

Figure 2.2: *Concept of power-line communication where the top image depicts data transfer over CAN bus while the bottom image depicts data transfer over the power grid instead. As seen, the number of cables is reduced in the latter case.*

As with every communication system both signal generation and the channel through which the signal propagates is equally important in PLC. Sections 2.1 to 2.3 provide brief explanation about digital signal processors and basic digital communication system . Sections 2.4 and 2.5 provide brief explanation about some aspects of system identification and stochastic signal processing used for channel and noise modelling respectively.

2.1 Digital Signal Processor

Digital signal processing chips (DSP) were introduced in the early 1980's and they differ from ordinary microprocessors in that they are designed for performing sum of products operation required in discrete-time signal processing as they contain hardware parallel multipliers [7]. There are two types of DSPs available, either with fixed- and floating-point number representation. The difference is in how the data is represented and computed.

In fixed point representation the data is represented as a normal integer. However, instead of interpreting the number as its integer value it can for example be considered as equal steps between -1 and 1. A signed 16 bit integer has a maximum value of 2^{15} - 1 = 32767 and a minimum of -2^{15} = -32768. Since the steps between these are integer values, considering the maximum value as 1 and minimum as -1 renders equally divided steps within the given range. The steps are calculated by simply dividing 1 by the number

of bits, such as 1 / 2^{15} = 0.0000305 [17].

When it comes to floating-point, the data is represented in a different way. The name floating-point is based upon the fact that the spacing between the values are not evenly distributed. With larger numbers the distance increases while it decreases in the case of smaller ones. A floating-point number consists of three parts: the first bit is the significand that tells if the value is positive or negative, it is followed by the mantissa which represents the coefficient, finally there is the exponent. The number is then represented by multiplying the significand with the mantissa raised by the exponent [18].

Floating-point representation has a number of advantages over its fixed-point counterpart, such as higher precision, better dynamic range and lower development time, while the main advantage of a fixed-point representation is the lower hardware cost which. What the floating-point processor does better is to achieve a higher signal-to-noise (SNR) value, since the spacing between numbers is smaller than that of fixed-point, resulting in reduced standard deviation within the quantization noise. A floating-point DSP has about 3000 times less quantization noise than a fixed-point DSP [19]. In this project we preferred fixed-point hardware over floating-point hardware as cost minimization was crucial from company's perspective.

2.2 Open Systems Interconnection model.

Open Systems Interconnection model (OSI) is a reference model founded by International Standards Organization (ISO) for the creation of new tasks, services for the development of new protocols and applications in a network consisting of several nodes and hosts [20]. The model is broken down the into seven different layers as shown in the Figure 2.3.

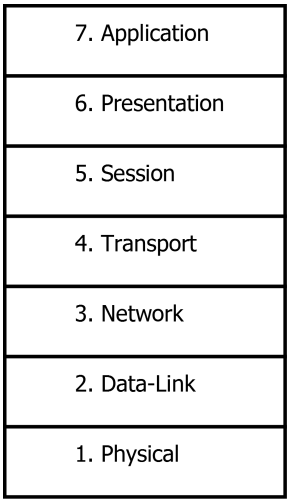

Figure 2.3: *Seven layers of OSI model.*

A brief description of each layer as described by Alpern et al. [21] is as follows, the physical layer represents the mechanical and electrical components required for the transmission of bits between two nodes and/or hosts in the network. The functions of data-link layer are formation of packets, management of frames, flow control, error notification

etc. Transport layer establishes logical connections between nodes and manages end-to-end flow control, error detection and recovery. Network layer represents the logical connection between two nodes/hosts. Session layer is responsible for monitoring and terminating sessions using the logical circuits formed by the transport layer. Presentation layer is responsible for data encryption and decryption including both data and protocol translation. Application layer represents user interaction with the network. In this project, we will be focusing only on physical and data link layer of the OSI model.

2.3 Digital Communication System

The need for digital communication systems is increasing continuously since, in most cases, the data to be transmitted is either in digital form or can be easily converted to digital form. Digital transmission systems have many advantages; namely cheap hardware, good control of quality and flexibility. They also offer additional security in comparison to the analog communication systems [22]. A basic block diagram of a digital communication system is shown in Figure 2.4.

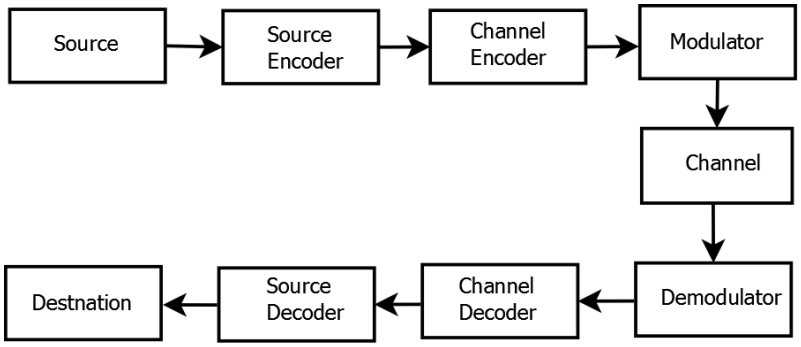

Figure 2.4: *Block diagram of a Digital Communication System.*

If the data to be transmitted is not available in digital form, it is obtained from an analog waveform with the help of sampling and quantization. Once the data is available in digital form, the purpose of the transmitter is to convert the data into a signal having finite (discrete) levels or continuous levels depending on the nature of the medium used for transmission. The conversion is performed with the help of a modulator. However, before passing the data into the modulator, it is modified by a source encoder and a channel-encoder. The source-encoder modifies the data in such a way that the data carries more information while maintaining the same data rate. The channel-encoder adds redundant bits so that it is easy for the receiver to decode the received signal with the least amount of errors. In the receiver the whole process is reversed and the demodulator converts the analog signal to digital form. This digital signal is subsequently passed through the channel decoder to remove the redundant bits before being passed through the source decoder which adds the extra bits that was removed in the source encoder.

2.3.1 Source Encoder

The source encoder compresses the transmission data depending on the probability of occurrence of ones and zeroes such that each bit carries more information. The data rate

at the output will usually be lower than the data rate at the input. The advantage of encoding the data is that the bandwidth of the signal is reduced.

2.3.2 Channel Encoder

The purpose of a channel-encoder is to safeguard the input data (information bearing sequence) against any possible distortion that may occur during the transmission over the channel, it is also referred to as error-control coding. The channel encoder adds additional redundant bits which helps the receiver to effectively recover the original bits from the received signal.

2.3.3 Modulator

The bit sequence must be converted to an analog signal before transmission, this is done with the help of a modulator. In baseband transmission, the data bits from the source are converted to a train of pulses which is also known as baseband signal. The pulse-shape used to form the pulse-train is known in advance. One of the popular pulse shapes used in communication systems is the root-raised cosine (RRC) pulse-shape shown in Figure 2.5.

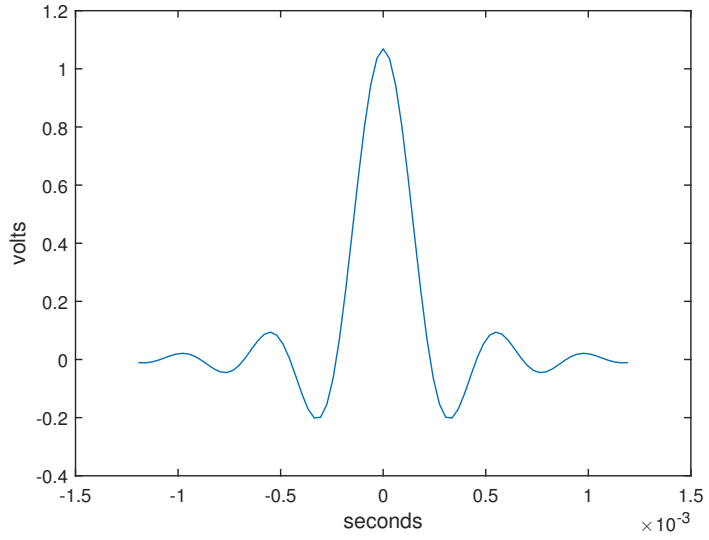

Figure 2.5: *Root-raised cosine pulse-shape.*

The root-raised cosine at a given instant t is defined by (2.1), where α is called the excess bandwidth factor and T is the sampling interval [22].

$$v(t) = \frac{sin(\pi t/T)}{\pi t/T} \frac{cos(\alpha\pi/T)}{1 - 4\alpha^2 t^2/T^2} \tag{2.1}$$

In passband transmission, the baseband signal is multiplied by a carrier wave of known frequency. Multiplying the carrier wave with the baseband signal in the time-

domain is equivalent to the convolution in the frequency-domain which results in a passband signal. The frequency of the carrier signal is chosen depending on the spectrum available for transmission. Finally, the passband signal is converted to analog form with the help of a digital-to-analog converter (DAC) and transmitted across the channel.

Modulation Scheme: Depending on the type of modulation used, the amplitude and/or phase of the pulse-shape described in the previous section is changed [22]. For example in binary phase-shift keying (BPSK) the amplitude is kept constant while the phase is changed by 180 degrees. If four-point quadrature amplitude modulation (QAM) is used, then both the amplitude and phase is changed. The modulation scheme determines the number of bits represented by a symbol. The time taken by a symbol is known as the symbol-time T_s, consequently the number of symbols at a given time is known as the symbol-rate R_s. The bit-rate and the symbol-rate change based on the type of modulation. The relation between time taken by a bit T_b and the number of symbols m is given by $T_b = \frac{T_s}{log_2(m)}$. The train of pulses which represent the bit sequence is known as the baseband signal.

2.3.4 Channel

In the real world different types of physical channels are present through which communication takes place. Channels are mainly classified as wired channels which include telephone lines, fibre-optic cables and power-lines; wireless channels which include satellite links and mobile communications; and recording media including compact discs and other electronic media.

2.3.5 Demodulator

The function of the demodulator is to estimate the bits from the received signal which is now combined with noise. The process begins by first converting the signal from the analog domain to the digital domain by sampling and quantization with the help of an analog-to-digital converter (ADC).

The first step in the demodulation is the downconversion of the received signal from carrier frequency to baseband which is a pulse-train. This is achieved by passing the signal through a low-pass filter. The train of pulses obtained from the filter is sampled at an integral multiple of the symbol-time T_s. This type of receiver is known as a sampling receiver [22]. The modulator detects the correct bits based on the location of the received samples in the signal space which is known with the help of signal constellation.

The received bits representing one of the symbols is chosen in a way such that it is closest to the sample at the given time in the signal constellation. If $y(t_i)$ is the sample obtained at time t_i then the selection of the received symbol is given by (2.2). This method of detection is known as the maximum likelihood estimation.

$$i = \arg \min_{i \in 1,\ldots,M} D_i, \quad where \quad D_i = |y(0) - s_i(0)| \tag{2.2}$$

2.3.6 Channel and Source Decoders

The output from the demodulator is a sequence of bits. However, the sequence includes redundant bits that carry no information which were added by the channel encoder to improve the detection at the receiver. The function of the channel decoder is to remove these additional bits. The function of the source decoder is to perform the reverse operation that was performed by the source encoder enabling the data use at the destination.

2.4 System Identification

It is often required to describe a physical system mathematically since mathematical relations provide a clear picture of how different factors affect the system. According to Keesman [23], system identification helps to estimate a mathematical model of a given system based on the data observed from the same system. A mathematical model is a mathematical structure or a set of equations used to capture a generalised behaviour of a system or a signal under consideration at a certain abstraction level. A mathematical model is always an approximation of a real system. The system identification procedure involves four main steps, namely:

1. Data acquisition
2. Selection of the model set based on the acquired data and estimation of parameters
3. Model validation

There are two types of models in system identification: parametric and non-parametric models. The parametric models assume a certain structure to the model before estimation, then the parameters of the assumed structure is estimated such that input and output are closely related. The estimation is performed by reducing the mean-squared error between the estimated output of the model and the actual data set obtained from the system under consideration. Non-parametric models on the other hand do not assume any specific structure to relate the input and output to describe a system, examples of the non-parametric model include impulse response and frequency response [24].

2.4.1 Model

In this project, we have used the autoregressive with external input (ARX) method has been utilised to estimate the model of the channel. The following set of equations provide the basic idea behind ARX as described by Ljung [24]. In general, the input *u(n)* and output *y(n)* of a system can be described by the linear-difference (2.3) since the sampled data considered is discrete in nature.

$$y(n) + a_1 y(n-1) + ... + a_p y(n-p) = b_1 u(n-1) + ... + b_q u(n-q) \tag{2.3}$$

$$y(n) = -a_1 y(n-1) - ... - a_p y(n-p) + b_1 u(n-1) + ... + b_q u(n-q) \tag{2.4}$$

Introducing vectors,

$$\theta = [a_1...a_p \quad b_1...b_q]^T \tag{2.5}$$

$$\varphi(t) = [-y(n-1)... - y(n-p)) \quad u(n-1)...u(n-q)]^T \tag{2.6}$$

Using (2.5) and (2.6) within (2.4) the result becomes,

$$y(n) = \varphi^T(n)\theta \tag{2.7}$$

From (2.4), it is clear that the current output is obtained, given that the parameters in θ are available, hence the above equation can be written as,

$$\hat{y}(n|\theta) = \varphi^T(n)\theta \tag{2.8}$$

2.4.2 Least Squares Method

In order for the estimated model to fit the actual data, the value of the parameters in θ has to be adjusted. Least Squares Method [24] is used to find the minimum values of the parameters in θ such that $\hat{y}(n|\theta)$ approaches *y(n)*.

$$\min_{\theta} \; V_N(\theta, Z^N) \tag{2.9}$$

where,

$$Z^n = \{u(1), y(1), ..., u(N), y(N)\} \tag{2.10}$$

and,

$$V_N(\theta, Z^N) = \frac{1}{N}\sum_{t=1}^{N}(y(t) - \hat{y}(t|\theta))^2 = \frac{1}{N}\sum_{t=1}^{N}(y(t) - \varphi^T(t)\theta)^2 \tag{2.11}$$

$\hat{\theta}_N$ is the value of θ as described by (2.9),

$$\hat{\theta}_N = \arg\min_{\theta} \; V_N(\theta, Z^N) \tag{2.12}$$

Since V_N in (2.11) is quadratic, its minimum value is found by setting the derivative to zero. The resulting equation becomes,

$$0 = \frac{d}{d\theta}V_N(\theta, Z^N) = \frac{2}{N}\sum_{t=1}^{N}\varphi(t)(y(t) - \varphi^T(t)\theta) \tag{2.13}$$

After simplifying the above equation the result becomes,

$$\hat{\theta}_N = \left[\sum_{t=1}^{N}\varphi(t)\varphi^T(t)\right]^{-1}\sum_{t=1}^{N}\varphi(t)y(t) \tag{2.14}$$

Once the data is sampled and the vectors are defined, the solution can be determined using Matlab.

2.5 Discrete-Time Stochastic Process

The real world consists of signals which are either deterministic or random as well as signals that are both deterministic and random (pseudo-random). It is important to know how to analyse random signals similar to deterministic signals. However, some basic definitions with respect to random signal analysis must be known before proceeding to the actual study of the methods, these definitions are listed briefly below.

- **Experiment**: A procedure which when performed generates some results.
- **Outcome**: A possible result of an experiment.
- **Event**: Set of outcomes of an experiment.
- **Sample space**: Sample space can be considered as the universal set of possible outcomes from an experiment.

Given an experiment E, a random variable $X(\xi)$ is a real valued function such that X maps to every possible outcome from the sample space S ($\xi \in S$), such a random variable is known as a continuous random variable. If the random variable maps only to a finite or countably infinite number of values, then X is referred to as a discrete random variable [25].

A stochastic process is a collection of random variables indexed by time. In a stochastic process, if each random variable sampled at discrete instants of time has a discrete value, then the given stochastic process is referred to as a discrete-time stochastic process.

For the remaining theory, consider that *x(n)* is a sampled version of a continuous signal *x(t)* sampled at time instants $t{=}nT$, where T = sampling period and n = *0,1,2...N-1*. Some of the functions and quantities which makes the study of random signals simple are listed below.

- **Probability**: The probability of an event provides the quantitative measure of occurrence of the given event and is defined as $P(event) = \frac{event}{total\ number\ of\ outcomes}$
- **Probability Distribution**: A probability distribution is a function which assigns probability to each and every outcome of a discrete random variable.
  If, outcomes=$\{\ x_1, x_2, x_3, ..., x_N\ \}$ then the probability distribution is given by
  F(x)=$\{\ p(x_1), p(x_2), p(x_3), ..., p(x_N)\ \}$.
- **Mean**(μ): The mean, also known as the expected value *E(x)* of a distribution, signifies the central value of the given probability distribution and is defined by $\mu = E(x) = \sum_{i=0}^{N} x_i p(x_i)$.
- **Variance**(σ_x^2): The variance of a distribution signifies the spread of the given distribution around the mean value and is defined by,
  $\sigma_x^2 = \sum_{i=0}^{N} (x_i - \mu_x)^2 p(x_i)$.

- **Auto-correlation function**($r_x(k)$): The auto-correlation function is used to determine the correlation between values from different instants in time of a random process. The auto-correlation function of a random process is defined by, $r_x(k) = E(x(n)x(n-k))$.
- **Power Spectral Density(PSD)**: The PSD describes how the values of a random process is distributed over frequency.
- **White Noise**:The white noise is a sequence of uncorrelated random variables having constant variance. In order to do noise modelling, the most common type of noise-model used is the Additive White Gaussian Noise (AWGN) [25].

2.5.1 Spectral Estimation

Similar to deterministic signals, when a stochastic process is given as the input to an LTI system the output is also a stochastic process, provided the given system is stable [25]. This property can be used to estimate the spectral properties of a random signal.

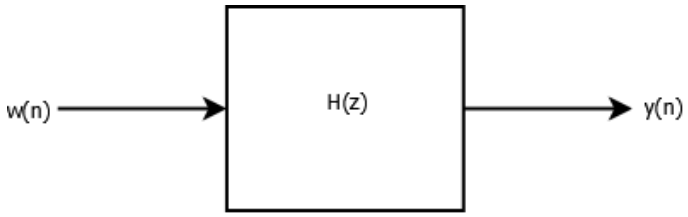

Figure 2.6: *Filtering white noise with a digital filter.*

Consider the filter shown in Figure 2.6, the output *y(n)* can be written as,

$$y(n) = \sum_{k=-\infty}^{\infty} h[k]w[n-k] \tag{2.15}$$

Then it can be shown that the input and output power spectra are related as,

$$P_y(e^{jw}) = \left|H(e^{jw})\right|^2 P_w(e^{jw}) \tag{2.16}$$

In the above equation, if the white noise has a variance of σ_w^2 which is equal to its power, the above equation can be written as,

$$P_y(e^{jw}) = \left|H(e^{jw})\right|^2 \sigma_w^2 \tag{2.17}$$

From the above equation we can infer that if the filter is stable then we can use this equation to model the spectrum of the stochastic process. According to the spectral factorization theorem, all the smooth spectra can be estimated with the help of a filtered white noise with a sufficiently higher order filter. Considering the transfer function of the filter as,

$$H(z) = \frac{B(z)}{A(z)} \tag{2.18}$$

where,

$$B(z) = 1 + b_1 z{-}1 + ... + b_q z{-}qA(z) = 1 + a_1 z{-}1 + ... + a_p z{-}p \tag{2.19}$$

If the above equation is converted into a difference equation, the result becomes,

$$y[n] + a_1 y[n+1] + ... + a_p y[n-p] = w[n] + b_1 w[n] + ... + b_q w[n-q] \tag{2.20}$$

Equation 2.20 is known as the autoregressive-moving-average (ARMA) process. A special case of the ARMA process is the AR process which consists only of poles(q=0). Then (2.20) becomes,

$$y[n] + a_1 y[n+1] + ... + a_p y[n-p] = w[n] \tag{2.21}$$

consequently, the spectra of the AR process is given by,

$$P_y(e^{jw}) = \frac{\sigma_w^2}{|A(e^{jw})|^2} \tag{2.22}$$

The autoregressive (AR) process models are favoured when the spectrum to be estimated consists of more peaks since it is an all-pole configuration. Another special case of the ARMA process is the moving-average (MA) process models favaoured when the spectrum consists more valleys than peaks. In this project we will be using only AR process and the next step is to find the procedure to determine the coefficients and this is done with the help of the Yule-Walker equation given below [25], [26].

$$r_y[k] + \sum_{l=1}^{p} a_l r_y[k-l] = \sigma_w^2 \delta[k], k \geq 0 \tag{2.23}$$

where $\delta[k] = 0$ for $k \neq 0$, *k=0,1,..p* and $r_y[k]$ is the autocorrelation function of the output. Using the matrix method shown below we can determine the coefficients provided we have the autocorrelation functions.

$$\begin{bmatrix} r_y[0] & r_y[1] & \cdots & r_y[p-1] \\ r_y[1] & r_y[0] & \cdots & r_y[p-2] \\ \vdots & \vdots & \ddots & \vdots \\ r_y[p-1] & r_y[p-2] & \cdots & r_y[0] \end{bmatrix} \begin{bmatrix} a_1 \\ a_2 \\ \vdots \\ a_p \end{bmatrix} = - \begin{bmatrix} r_y[1] \\ r_y[2] \\ \vdots \\ r_y[p] \end{bmatrix} \tag{2.24}$$

2.5.2 Welch's Method

One of the most common methods for estimating the PSD of a random signal is the periodogram. The periodogram of a random process is given by the discrete-time fourier transform (DTFT) of an autocorrelation function of the given random process,

$$P(e^{jw}) = \sum_{n=-\infty}^{\infty} r_x[n] e^{jwn} \tag{2.25}$$

where $\omega = \frac{2\pi}{T}$ is the digital frequency in radians per sample and T=sampling interval. However, the periodogram has some disadvantages such as that the frequency resolution is proportional to the sample length which requires large data to obtain a better estimation as well as a high frequency masking (refer Section A.6). These disadvantages can be reduced by using Welch's method to estimate the PSDs. Welch's method is basically averaging the periodogram. This is achieved by overlapping segments for improving the frequency resolution. Additionally, the requires less number of samples than the actual periodogram to estimate the PSD. It essentially calculates the periodogram for small segments, and uses a well chosen window function to achieve better variance.

3

Methodology

The project consisted of literature studies within the field of PLC where the focal point of the study has been upon IEEE articles on the subject, but other sources have occasionally been utilised as well. These are listed within the bibliography. The work was carried out in two parallel paths. One path was to implement the modulation and demodulation algorithms into a fixed-point processor and evaluating the impact of rounding errors compared to a floating-point implementation in Matlab. The second path was to model a channel as realistically as possible to that of an actual vehicle. To model the channel, both measurements in a lab environment as well as noise measurements in a real truck were made.

The quality of transmission depends not only on robustness and speed of the algorithms but also on the channel characteristics. Therefore, both algorithm design and channel modelling are of great importance in the procedure of evaluating the constraints related to vehicular PLC. This project focuses on the aspects of fixed-point representation and channel modelling, and will lay a necessary foundation for future work to build upon.

3.1 Implementation

Using a fixed-point processor has advantages like minimum cost, increased speed but with loss of precision. The processor that was chosen was the DSP TMS32C5515 from Texas Instruments (TI). For more details on the processor please refer to the data sheet [27].

Apart from the processor itself, a digital-to-analog converter (DAC) is required to convert the digital signal to the analog domain. The DAC that was chosen for this purpose was AD5686R [28] from Analog Devices. Three properties in specific were desired with the DAC: serial peripheral interface (SPI) for communication, 16-bit data conversion, and conversion a high speed. In order to convert the analog signal back to digital form an ADC is needed. However, the DSP itself has an integrated ADC which was used so there was no extra hardware required for this purpose.

For the implementation, two pieces of software were required. The first one needed to be able to test and verify the algorithms that were being used. For this purpose Matlab has been used. Matlab is a widely used software for mathematical calculations and the wide range of built in functions makes it a perfect option to simulate algorithms used for digital transmission, as in the case of this project. The second piece of software was used to implement the algorithms onto the DSP with C code. As mentioned earlier, this software

was one of the reasons for choosing the selected DSP. The software is code composer studio (CCS) from TI. CCS is an integrated development environment (IDE) based on the open source IDE Eclipse [29]. The reason that CCS was a deciding factor in choosing the DSP is that it offers real time debugging which makes it possible to view variables while a program is being executed.

As mentioned earlier, the purpose of the implementation was to evaluate the feasibility of using fixed-point arithmetics for the digital transmission algorithms. To do this, a basic setup for the DSP was needed. This setup involved just a few steps: the DSP sampled the signal with the use of timer interrupts to make a transfer through SPI, then the DAC converted the data into an analog signal, which was then received at the ADC of the second DSP which made a conversion back into the digital domain.

The peripherals used for SPI, timer interrupts and ADC in the DSP needed to be configured in order to make the signal chain possible. A short explanation of how these peripherals were configured is given in Appendix A.2. Finally the output from the Matlab implementation was compared side by side with the fixed-point implementation in the DSP.

3.2 Channel Modeling

The channel measurements have been done with both the use of a lab setup and a real truck. In the lab environment, the transfer characteristics of a set of wires was to be obtained, while noise was to be measured and evaluated from the truck.

The setup used to obtain the data from the channel should be as close to an actual vehicle as possible. However, reproducibility is desired in the lab environment which makes a simpler setup than an actual vehicle required. In a car the chassis serve as ground for the electrical system, for the lab environment two metal sheets were used to replicate the grounding in a vehicle. Optimally a sheet with the size of that in a car should be used, however that was not practically possible in the lab. The size used for each metal sheet was 1000 x 500 x 1.2 mm, which approximately was 2000 x 500 x 1.2 mm when combined.

To further mimic the environment of an actual car, a car battery with 12 volts was used to provide the DC voltage onto the channel. The battery also powered a load that was switched by a relay at given intervals. The relay that was used was of a solid state type and was chosen due to that it could operate at currents of up to 30 amperes. The channel itself contained a single copper wire of different length and thickness for different test scenarios. The setup used can be seen in Figure A.1.

Two signal generators were used to provide a signal. The signal generators that were used were two 33120A from Agilent, synchronised with a common trigger pulse. To measure the signal, a digital oscilloscope from Rigol DS2072A was used, it can measure signals up to 50 MHz with 1 GS/s and has a convenient USB interface to store samples onto a PC. Please refer to Appendix A.4 for the settings of the oscilloscope at the time of measuring.

3.2.1 Setup for Channel Measurements in Lab

Two types of measurements have been made in the lab. One to only measure the frequency response of the channel as a single wire, and one with a switching load connected. The setup in both cases consists of a metal sheet that serves as a ground plane comparable to that of a chassi in a car. In order to observe the switching transients a setup similar to that displayed in Figure 3.1 was used. The 50 Ω resistor parallel to the 470 kΩ resistor acts as the load. The purpose of this setup was to measure the fluctuations occurring across the wire while switching the load.

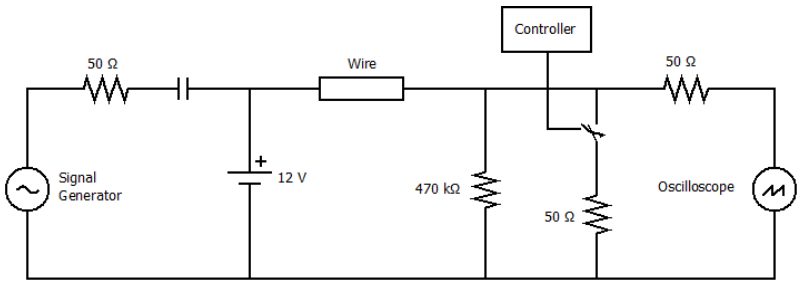

Figure 3.1: *Circuit diagram of the setup used for measuring the voltage fluctuation during switching.*

The two signal generators were synchronised by a common sync signal. One of the signal generator served as input to the channel and the other was used as a reference to the output from the channel. They were configured to generate square waves for the case without switching and a sine wave for the case with switching. The signals were sampled in the oscilloscope and stored to a computer where the original signal was compared to that which went through the channel. This was performed for various scenarios with different cable lengths and thicknesses. Utilizing the results of the measurements, a transfer function was computed.

A number of different test cases have been made for the measurement of the channel with three different wire configurations: 1 meter straight line, 2 meter straight line and 7.25 meter curved for each of the wire thicknesses namely 4, 10, 16, 20 american wire guages (AWG). Figure A.2 illustrates the wire configurations.

3.2.2 Setup for Noise Measurements in Truck

To measure the noise in the real truck, two parts of hardware were used, namely an oscilloscope and a breakout box. The oscilloscope used was TBS 1052B-EDU from Tektronix. Please refer to Appendix A.5 for the settings used during the measurement. To be able to access different nodes in the power grid, we used the breakout box provided by Volvo.

The noise was measured in a truck at Volvo Trucks facilities in Lundby, Gothenburg. The oscilloscope was connected to a node in the power line of the truck. In order to remove the DC component from the measurement, the coupling in the oscilloscope was switched to AC. The signals were measured at various points in the vehicle such as at the direction indicators, position lights and brake lights when the engine was ON since that is when noise is most present. All the samples were transferred to the computer for further analysis.

4

Channel Model

In every transmission system the channel plays an important role since, in most cases, it determines the data that can be transmitted in the presence of noise. Therefore it is important that the channel is represented by a mathematical model.

In the case of PLC, the entire power grid or, in this case, the wiring harness of the vehicle including the chassis acts as the channel. Chassis acting as the ground in a vehicle poses many complications to PLC. In any electrical circuit the path of the return current is the path of least resistance, but this is only true at lower frequencies. In the case of higher frequencies the current takes the path of least impedance, which is also the case in the wiring harness of a vehicle. The impedance is highly variable due to the presence of variable loads connected to the wiring harness. It would thus be incorrect to model the channel just assuming the path of least resistance [10].

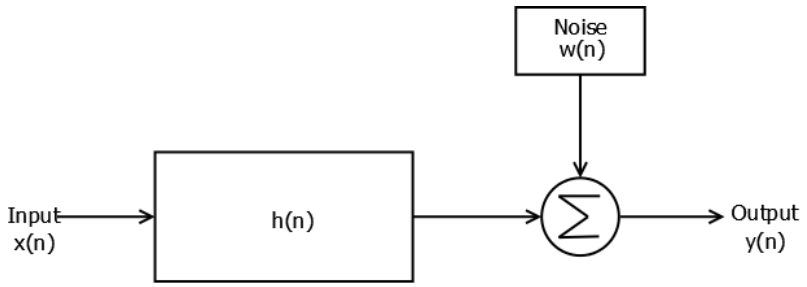

Figure 4.1: *Proposed model for the channel. Where h(n) represents the impulse response of the channel and Noise represents the disturbances from different sources.*

In this project we have used system identification methods to estimate the transfer function for different wires and wiring configurations found in a vehicle. As explained in Section 2.4, the system identification process begins by the collection of data. The quality and the information available in the data dictates the correctness of the model. Once the model is estimated using the available data it is validated using another set of data to check its correctness. The channel was modelled as an linear time-invariant (LTI) system along with noise as shown in Figure 4.1. In the first section the transfer function H(z) is obtained, and in the second the approximate model for noise w(n) is estimated.

4.1 Data Collection

The collected data is sampled data of the output for a known input at a given time. Since the data does not reflect any physical considerations in the wire, the model was estimated using black-box modelling approach [24]. One of the common black box modelling techniques is the ARX method explained in Section 2.4. The accuracy of the estimated model depends on how well the acquired data represents the different characteristics of the system under consideration.

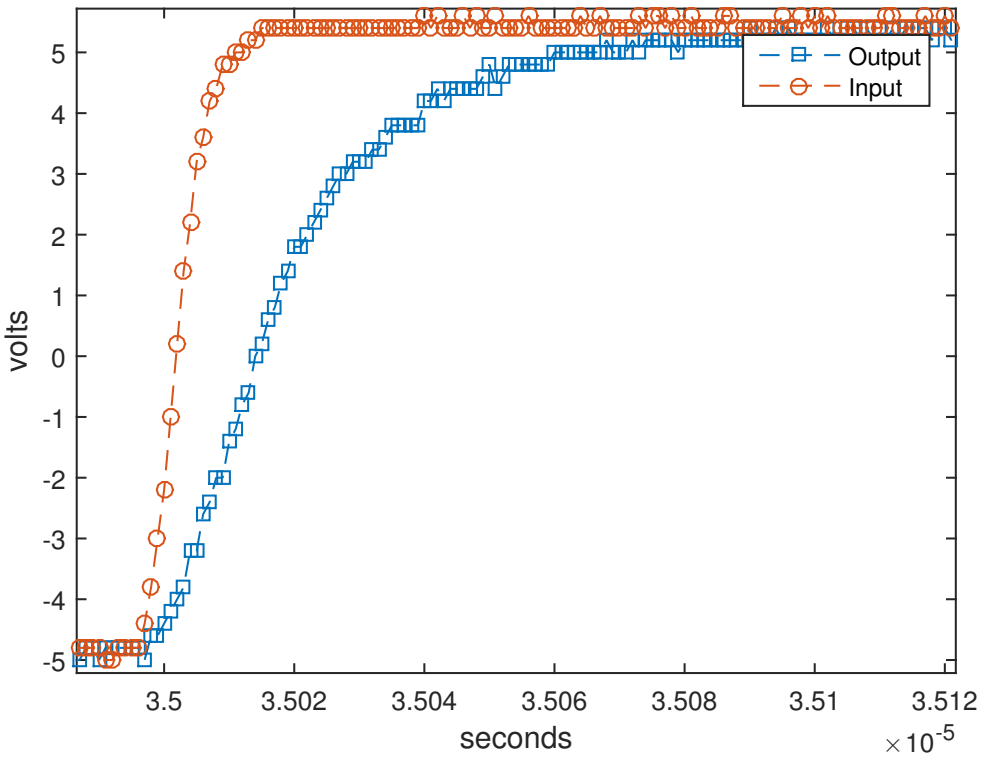

Figure 4.2: *Illustration of attenuation of high-frequency components for a step input.*

Initially, the data was collected at the output by doing a sweep from 10 Hz to 10 MHz of sinusoidal frequencies. However, due to the limited memory of the oscilloscope the entire range of frequencies could not be captured. To circumvent this problem, square waves were transmitted as each step of a square wave comprised of wide range of frequencies. Figure 4.2 shows the sampled input and output signals, it can be observed that sharp edges which represent high frequency components are being attenuated. The reason could either be the electromagnetic interference (EMI) from the surroundings or that the channel itself acts like an low-pass filter.

Once the data was sampled, the analysis and model estimation was performed with the help of Matlab. Since the model estimation is done offline it is difficult to emulate the real world scenario.

Another challenge was to combine the variation of outputs as a consequence of

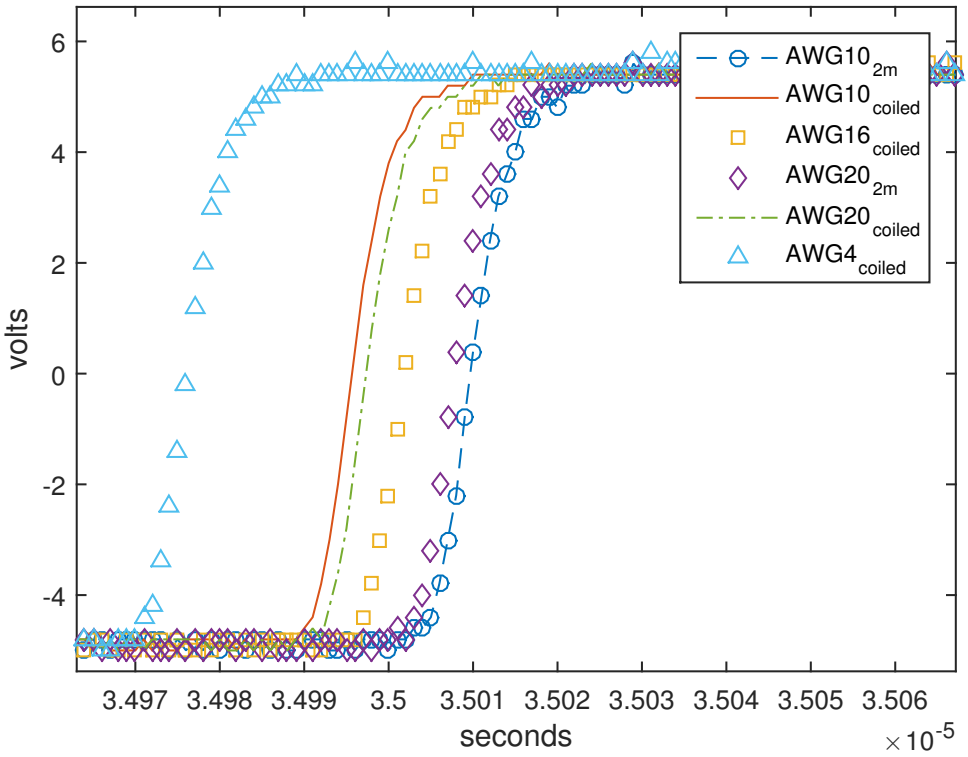

Figure 4.3: *Plot of the sampled data of a square wave at one of the edges for different wires.*

variation in lengths and thicknesses of the wires. Figures 4.3 and 4.4 show the variation in the output of multiple cases for different AWGs. Since the ARX model can only be estimated with observed data it does not reflect the actual physical system.

The data collected from the different experiments was concatenated into a single set and was used to estimate the model. This method provided a more general model rather than just estimating the parameters for a specific case of wire. It should be noted, that even by this approach the model is relatively far from the actual scenario found in vehicles, but it still provides a descent description of the system.

4.1.1 Transfer Function Estimation

The process of estimation begins by first selecting an appropriate structure for the transfer function. Once the structure is chosen, the estimation consists for finding the values of poles and zeroes of the transfer function. Therefore, a decision regarding the order of system as well as the number of poles and zeroes the transfer function must contain is crucial. Observing the collected data provided the insight that high frequency components are being attenuated, meaning that the channel is acting like an LPF. A multitude of differing combinations of poles and zeroes were investigated to estimate the coefficients. The calculated values of the coefficients were tested against a different set of data and the set of values which agreed with both data sets was chosen. The least-squares method described in Section 2.4.2 is used to estimate the coefficients to fit the actual data. The

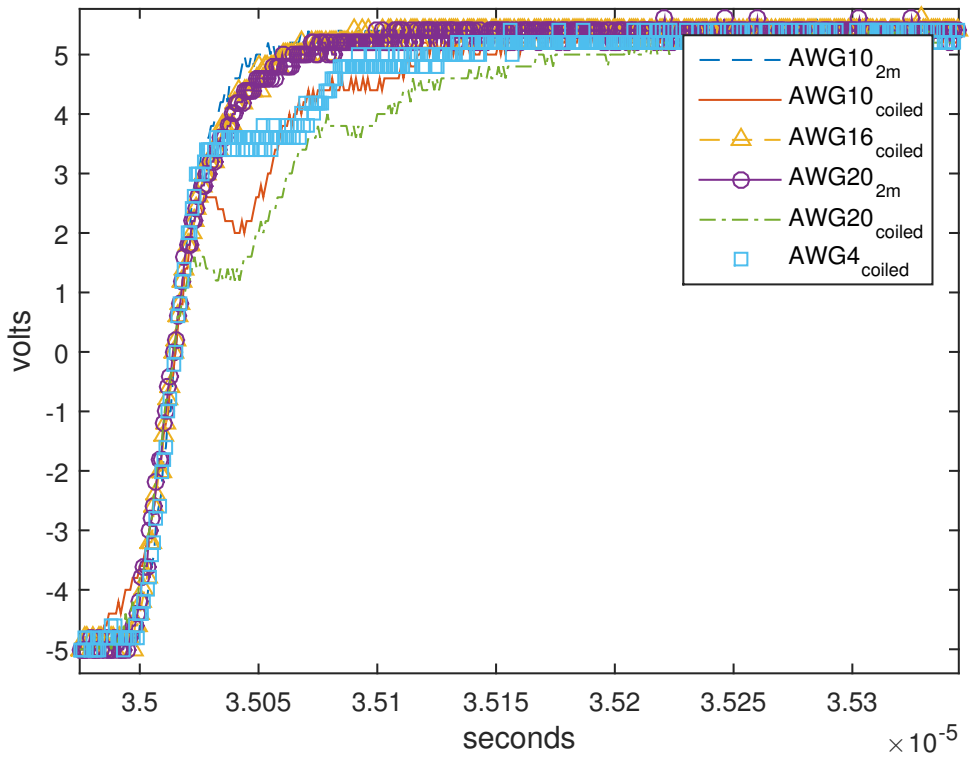

Figure 4.4: *Illustrating the variation in the attenuation of high frequency components for the input step signal shown in Figure 4.3.*

transfer function of the estimated model is given by (4.1).

$$H(z) = \frac{0.1821z^{-1}}{1 - 0.2759z^{-1} - 0.1013z^{-2} - 0.4397z^{-3}} \tag{4.1}$$

The bode plots of the transfer function is shown in Figure 4.6. From the figure it can be observed that the channel acts like an LPF with a cut-off frequency of 14 MHz.

4.1.2 Model Validation

As explained in Section 2.4, model validation is important to verify the correctness of the model. For this purpose, a second data set similar to the one shown in Figure 4.5 was used to validate the estimated model given by (4.1). The estimated model fits the validation data by 95.78%, shown in Figure 4.7.

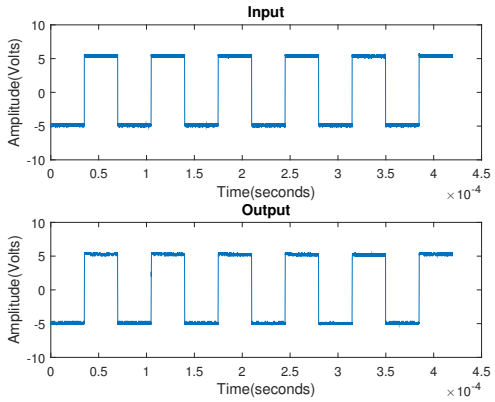

Figure 4.5: *Concatenated data which includes input and output data from different wires with varying thickness and lengths.*

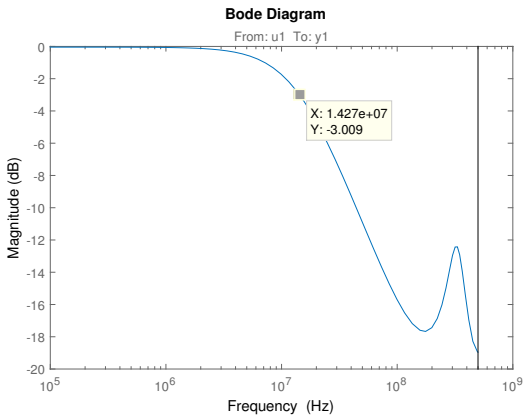

Figure 4.6: *Bode plots of the transfer function of the estimated transfer function given by the (4.1).*

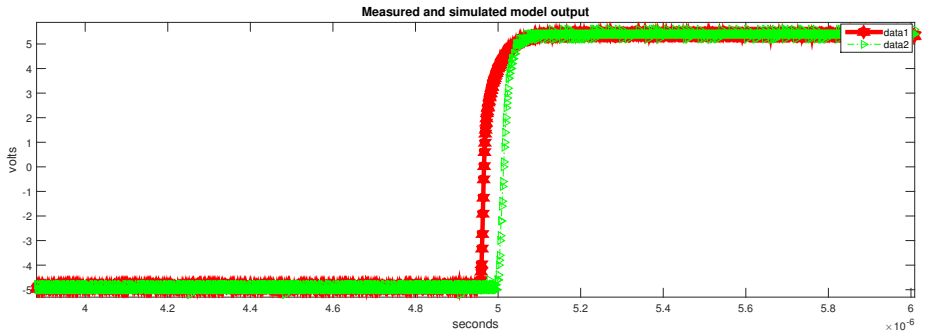

Figure 4.7: *Illustration of how well the estimated model fits the validation data. Data1 (red) represents the curve traced according to the estimated model. Data2 (green) represents the validation data.*

4.2 Noise

As for any other communication system, the study of noise is important for signal transmission in PLC. In most cases, the transmitted signal will be corrupted by noise, particularly if the power spectrum of the noise overlaps the carrier signal's frequency. However, it is possible to establish a good transmission if transmission is performed at frequencies where the noise is less likely to affect the signal transmission.

As noise is a random signal or a stochastic process, it can be approximated either with the help of a model or by characterising it with some properties. In most cases a model is required to handle random signals for the purpose of estimation. Estimation is useful in many ways, in particular for predicting the future outputs, in which case adaptive algorithms can be implemented to more effectively reduce the noise. Essentially what is needed is the value of the next noise sample so that its effect can be nullified. For this to happen there is a need for a model which describes a computational rule for the estimation.

Usually it is easier to extract useful information in the frequency-domain rather than in the time-domain as it helps to determine the periodicities inherent in the data. For random signals, the PSD is used to characterise the power distribution with frequency. Therefore, the model for the PSDs of the noise data is estimated (depicted in Figure 4.11), rather than estimating a model for time-domain data. The estimation of PSDs can be

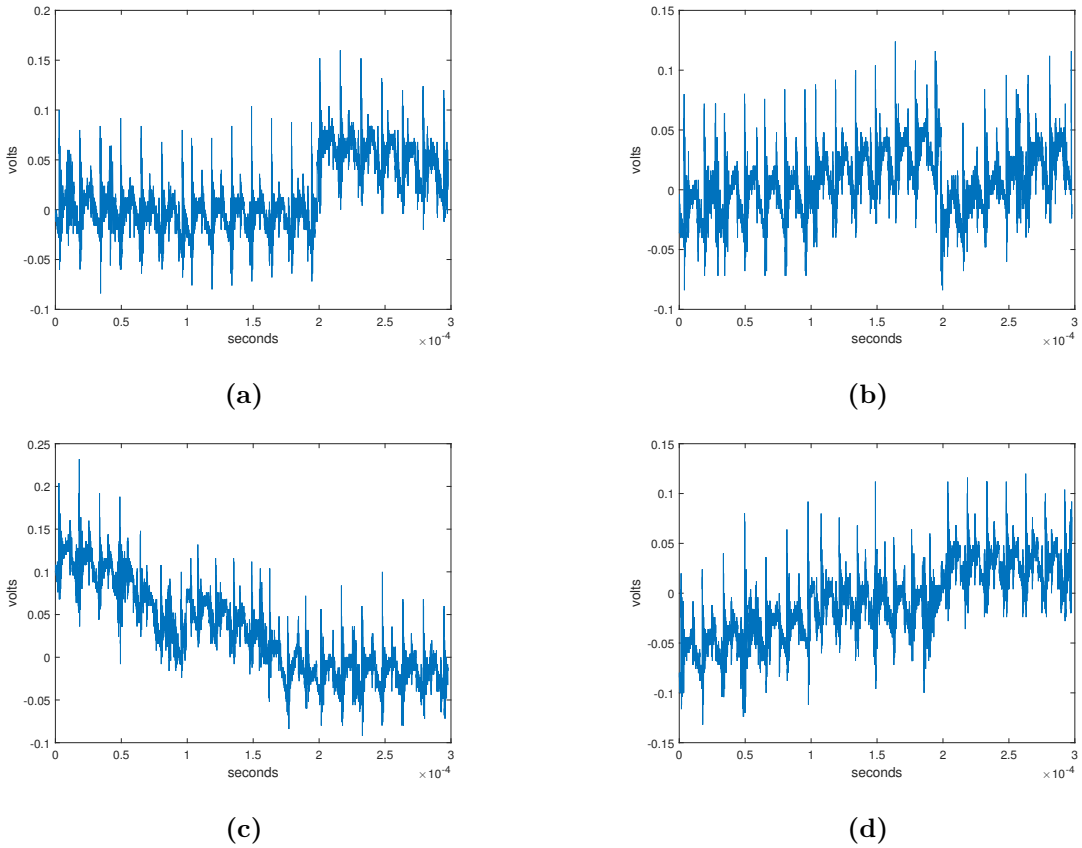

Figure 4.9: *Noise collected at different vehicle operation modes and different in a truck, (a): Position lights, (b): Position with turning indicators, (c): Position lights, turning indicators and braking, (d): Position lights, turning indicators, braking and wiper motor.*

performed by two methods, parametric and non-parametric estimation as described in Section 2.4.

In this project we used both parametric and non-parametric estimation has been utilised to estimate the PSD. The estimation of a model for a given stochastic process is executed in three steps:

1. Determining the stationarity, that is finding whether the given stochastic process is stationary or non-stationary.
2. Depending on the correlation between different data points, choosing a suitable model structure (AR, MA or ARMA).
3. Estimating the parameters for the chosen model structure.

The noise data is collected from a vehicle with the help of an oscilloscope. The procedure for acquiring data is described in detail in Section 3.2.2. All data samples were collected while the engine was running since noise is significantly higher while the engine is running, particularly the impulsive noise. The noise is increased further when there is a difference in load impedance due to switching of electrical appliances. Therefore the data samples were collected during different modes of operation, for example with position

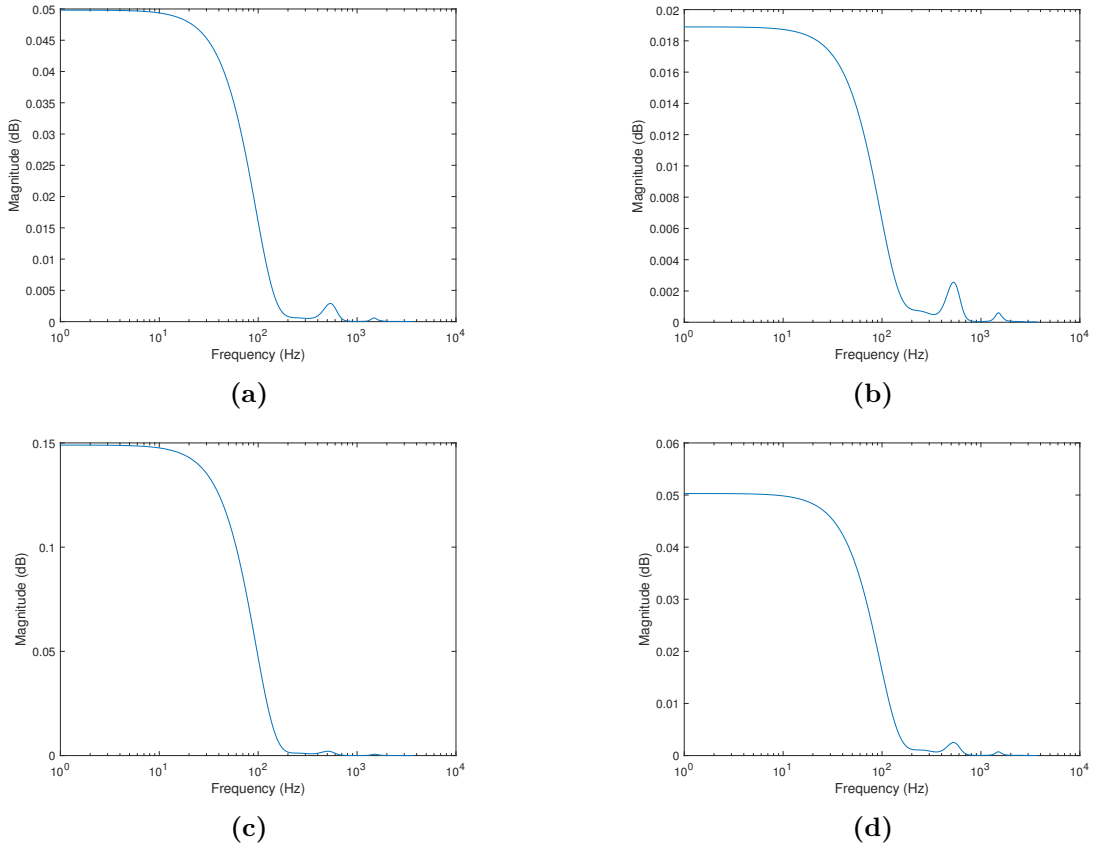

Figure 4.11: *PSD using Welch's method for the time domain data shown in Figure 4.9.*

lights, brake lights and direction lights. The time domain plots of the obtained data is shown in Figure 4.9.

Determining the stationarity of a stochastic process requires a large collection of data sets sampled at different intervals because assessing stationarity requires calculation of mean, variance and autocorrelation. Unfortunately, only a limited set of data was available. Therefore, we have assumed that the noise in this specific case is ergodic in mean to simplify the process of estimation. By assuming that a given stochastic process is ergodic in mean we can calculate mean of several realisations at a given instant of time using the a time average of any single realisation [25]. Thereby preventing the need to have a large set of data having many realisations. The next step in the estimation process is the selection of a suitable structure for the model so that the model can fit the data. The AR process, which is an all-pole system, was chosen for estimating the model. The selection was based on our Welch's estimate of the true spectrum which contained a multitude of peaks, as the AR-process estimates peaks better than valleys of a true spectrum [25], [26]. The plots in Figure 4.11 display the PSD estimate of the true spectrum using Welch's method. A ninth-order AR-process is chosen to obtain a proper fit for the data. The estimated model for the data shown in Figure 4.11 is as follows:

$$\begin{aligned} w(n) = {} & 1.0054w(n-1) - 0.2958w(n-2) + 0.2321w(n-3) + 0.0049w(n-4) \\ & + 0.0025w(n-5) - 0.1374w(n-6) - 0.1857w(n-7) - 0.0102w(n-8) \\ & + 0.3237w(n-9) + 1.03 * 10^{-4}e(n) \end{aligned} \tag{4.2}$$

where *e(n)* represents the white gaussian noise. Finally, the relation between output *y(n)* and input *x(n)* in Figure 4.1 is given by (4.3),

$$y(n) = x(n) * h(n) + w(n) \tag{4.3}$$

where *h(n)* represents the impulse response of the LTI system given by the inverse Z-transform of (4.1).

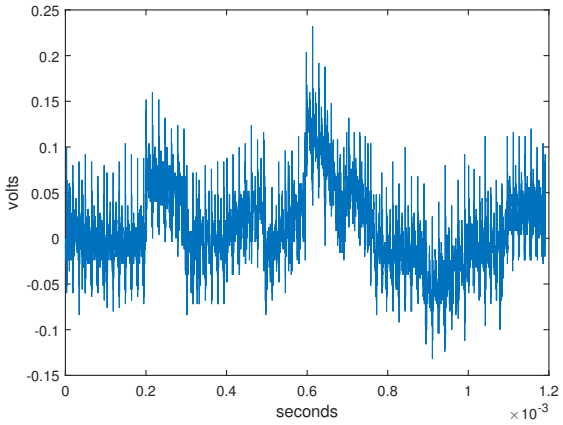

(a) *Plot of the concatenated noise data obtained from all the four cases shown in Figure 4.9.*

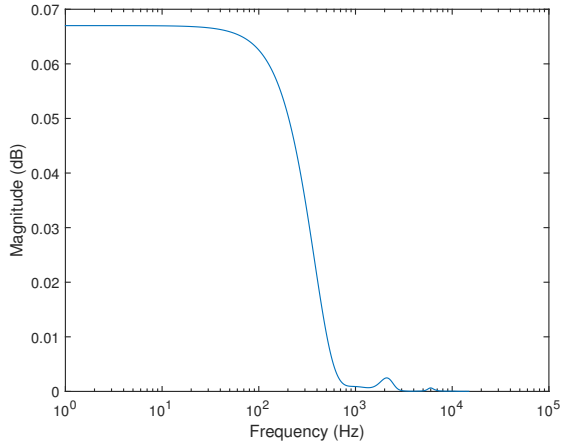

(b) *PSD of the above plot to obtain a better approximation using the AR-process.*

Figure 4.13: *PSD using Welch's method for the time domain data for all the four cases shown in Figure 4.9.*

4.3 Switching-Load Measurements

From the previous sections it is clear that all of the thicknesses and lengths of wires tested support frequencies up to 14 MHz. Additionally, the noise itself is not a problem as long the transmitted signal's amplitude is considerably higher. However, the effects of load impedance variation in the data used for modelling in the previous section remains unknown. Therefore, this section concerns how the output varies whenever the switching occurs with the help of the experiment described in Section 3.2.1. The input and output data at the point of switching is shown in Figure 4.14. The output is offset by 10 volts, this is due to fact that the DC voltage is not blocked during the measurement. It can also be observed that the output's peak-to-peak AC voltage is reduced to approximately half of the input AC voltage when the load is switched. This is because at the time of switching the stray capacitances increase. The current through and voltage across a capacitance is given by the relation below.

$$I = C\frac{\mathrm{d}V}{\mathrm{d}t} \tag{4.4}$$

When the switching takes place, there is a high influx of current through the load. But the rate of change of voltage $\frac{\mathrm{d}V}{\mathrm{d}t}$ remains the same in (4.4). Therefore it appears that there is an increase of the capacitance C. This increase in capacitance together with the wire resistance R will act as a low-pass filter and reduce the cut-off frequency of the entire channel. In Figure 4.14, only the input for two cases can be seen. Attempts utilizing

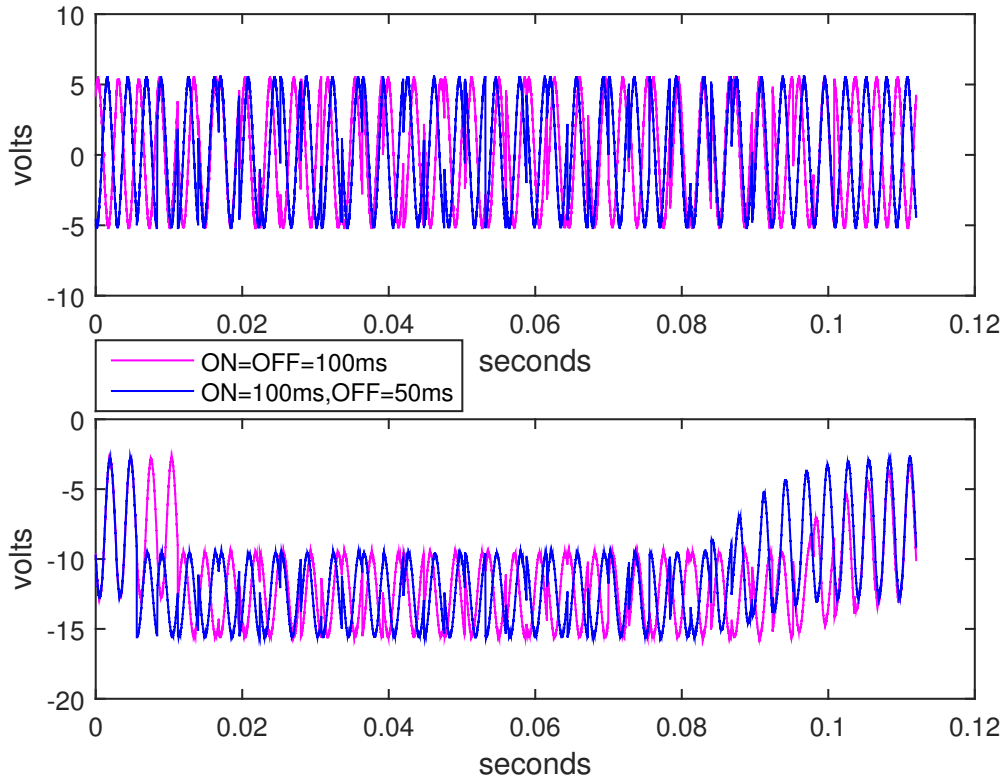

Figure 4.14: *The top graph shows the input signal of a 70 kHz sine wave for two cases with switching load, below is the output for the same cases. As seen there is attenuation of the signal when the switching occurs.*

different combinations of wire thickness, length and switching time all rendered similar results. A 50 Ω resistor was used as the load, but usually the load in an automobile is below 2 Ω, which means that the attenuation will be even worse in the wiring harness of a vehicle whenever switching takes place. This means that the switching activity will play a dominant role in inhibiting signal transmission.

5

Implementation

In order to study the effect of precision due to fixed-point representation, a functional prototype was needed. The eZdsp development platform from TI was chosen as it consisted of TMS320C5515, which is a fixed-point processor. For additional details about the hardware, refer to Section 3.1. One of the main issues with the fixed-point representation is the rounding errors introduced during each stage in the algorithm due to the limited dynamic range. We implemented both modulation and demodulation to analyse how the precision of the data defines the quality of demodulation that can be achieved at the receiver. We started by implementing BPSK since it is relatively simple to implement and makes the analysis of rounding error at each stage in the signal chain easier as well.

5.1 Algorithm

Algorithms for both the transmitter and receiver were created using Matlab in order to verify their correctness. These were later implemented on the DSP using fixed-point C code. The flow chart of the algorithms for both the transmitter and receiver are shown in Figures 5.1 and 5.2.

5.1.1 Transmitter

The data was fetched from the flash memory and sent in 64-bit frames. The data was assumed to be source- and channel-encoded. Our focus was only on the modulation since rounding errors are commonly introduced during modulation at the transmitter side [22]. The modulated signal was then transmitted with the help of the external DAC which has a resolution of 16 bits.

The frame of bits fetched from the flash was first mapped to a set of symbols resulting in a symbol sequence and, since BPSK modulation was utilised, the symbol set consisted of two elements, which in this specific case was -1 and 1. The symbol sequence was then convoluted with a pulse shape which in this case was a RRC pulse, resulting in a train of symbols. Both the pulse shape and the symbol sequence was upsampled before the convolution. The upsample factor is in general defined by the ratio of sampling rate to the symbol rate. Finally, the symbol is then multiplied by the carrier frequency.

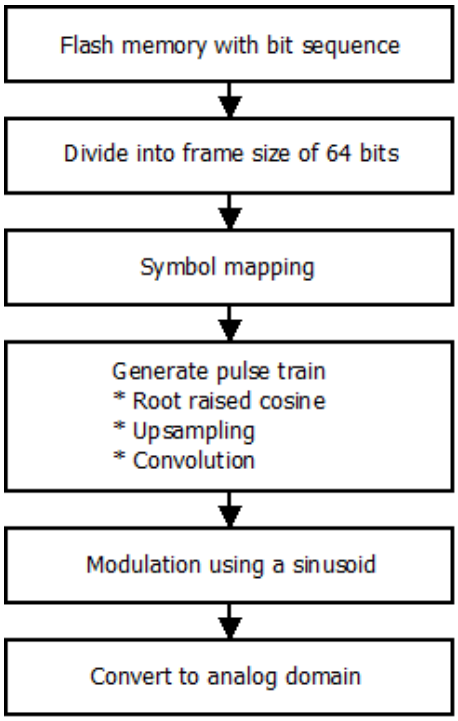

Figure 5.1: *Flow chart describing the operations within the modulator.*

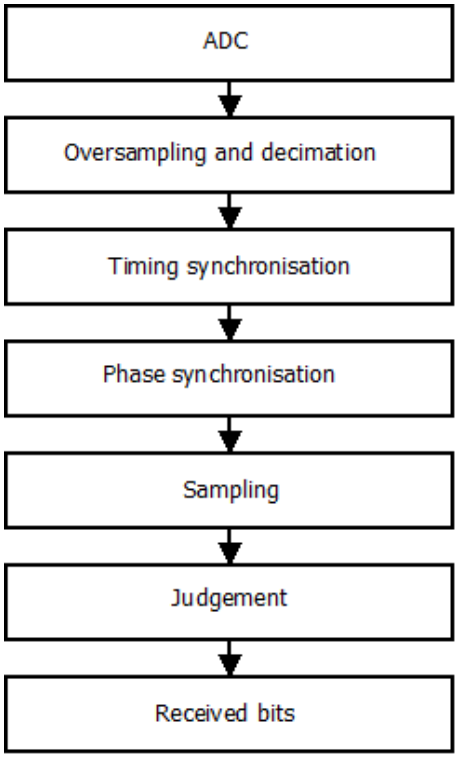

Figure 5.2: *Flow chart describing the operations within the demodulator.*

5.1.2 Receiver

In order to decode the signal it has to be converted from analog to digital form. At first there were issues in decoding the transmitted bits from the received signal because the ADC's resolution is merely 10 bits, which caused a reduction in the SNR to approximately 37 dB according to below.

$$SNR_{dB} = 6.02 * N + 1.76 \tag{5.1}$$

The equation gives the relation between the number of bits 'N' and SNR (dB) for a full-range sine wave [30]. The SNR is critical in the decision stage because there each sample is mapped to one of the symbols from the symbol set.

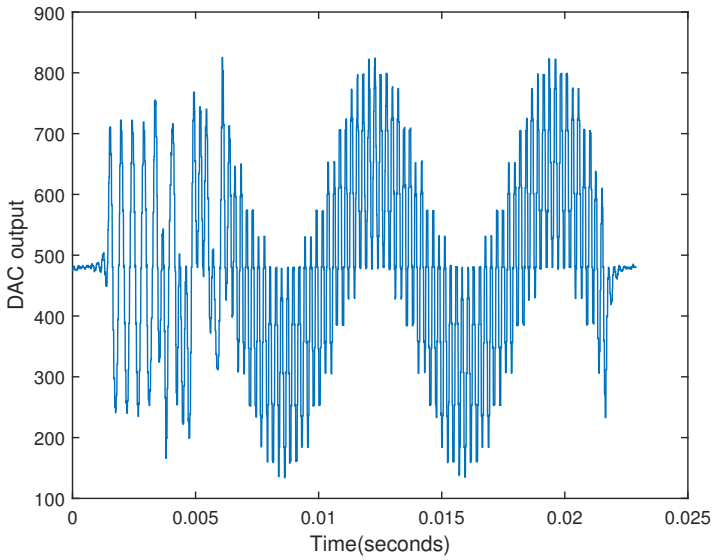

Figure 5.3: *Output from the 10-ADC, illustrating quantization error.*

The mapping is done depending on the minimum distance between the given sample and the different constellation points in the signal space. In order to increase the SNR, the incoming signal was oversampled by a factor of four. The oversampled signal can be seen in Figure 5.3. It was then decimated in two stages using half-band filters as shown in Figure 5.4.

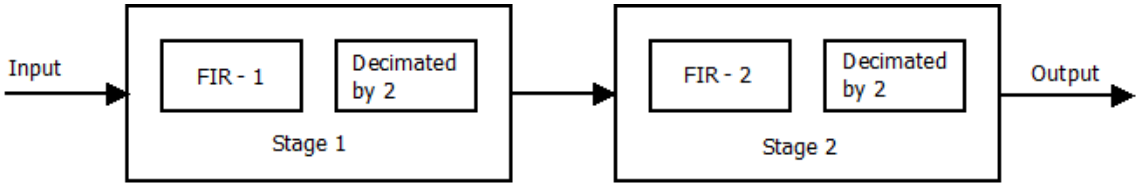

Figure 5.4: *Block diagram of the decimation stage for improving the SNR.*

Using half-band filters in each stage requires less coefficients than a single filter. The frequency-responses plots of the filters are shown in Figures 5.5 and 5.6.

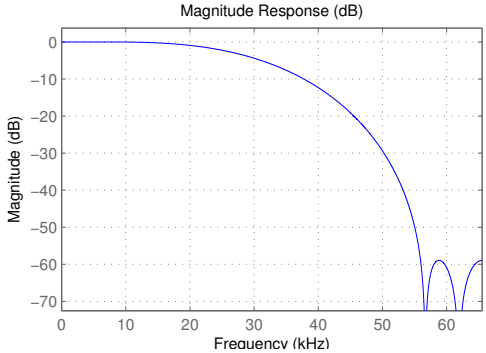

Figure 5.5: *Frequency response of the half band filter for a sampling frequency of 128 KHz.*

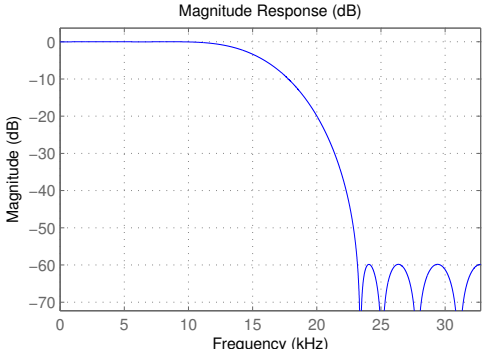

Figure 5.6: *Frequency response of the half band filter for a sampling frequency of 64 KHz.*

After decimation, it is required to apply a negative offset in order to extract phase information. The signal after decimation and offset is shown in Figure 5.7.

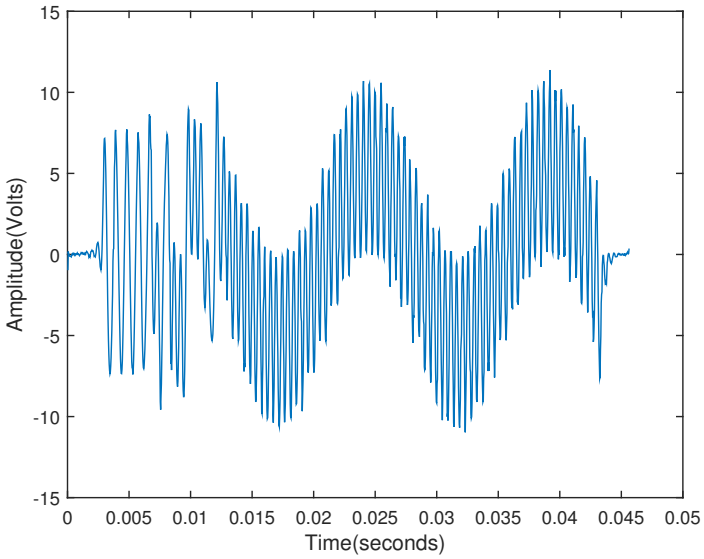

Figure 5.7: *Received signal after noise shaping.*

All the figures were generated with the help of Matlab but using the data obtained by accessing the memory of the processor with the help of code composer studio.

The receiver was designed as a sampling receiver to keep it simple, and therefore the timing and phase synchronization was critical. The timing and phase synchronization was achieved with the help of a preamble transmitted along the actual data. The timing synchronisation is achieved by correlating the received signal against a known sequence, in this specific case a barker code (refer Section A.6) was utilised. Following the time synchronization of the received signal, the phase synchronisation was achieved using a symbol with known phase present at a specific location in the preamble. The inverse trigonometric function was used to calculate the phase of each sample, in order to save memory, cordic algorithm was used to generate the values of the trigonometric functions. Once the received signal was synchronised in both time and phase, sampling was undertaken at regular intervals determined by the spacing between each bit in the received signal. The

correctness of the sampling was determined with the help of an eye diagram as seen in Figure 5.8. This shows the sampling instant of each bit. It is desirable to have a wider opening at the middle of the eye diagram. The wider opening signifies sampling of data at right intervals of time.

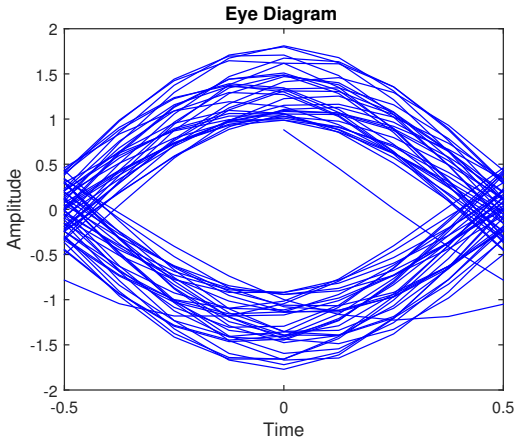

Figure 5.8: *Sampling times before judgement in BPSK, the widening of the eye at the middle clearly suggests that the sampling is done at the right instant.*

Figure 5.9 shows the pulse train with floating-point representation, while the rounding errors caused due to the fixed-point representation of data during modulation is shown in Figure 5.10.

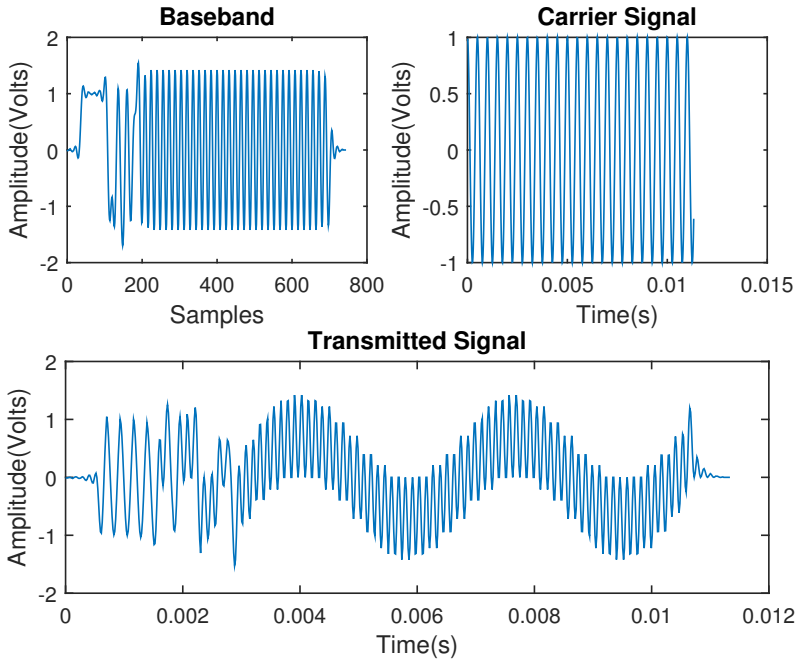

Figure 5.9: *The pulse train(baseband) and transmitted signal for preamble followed by a sequence of alternating ones and zeros using BPSK scheme on a 2kHz carrier.*

It is clear that the error is gradually increasing from the pulse-train generation

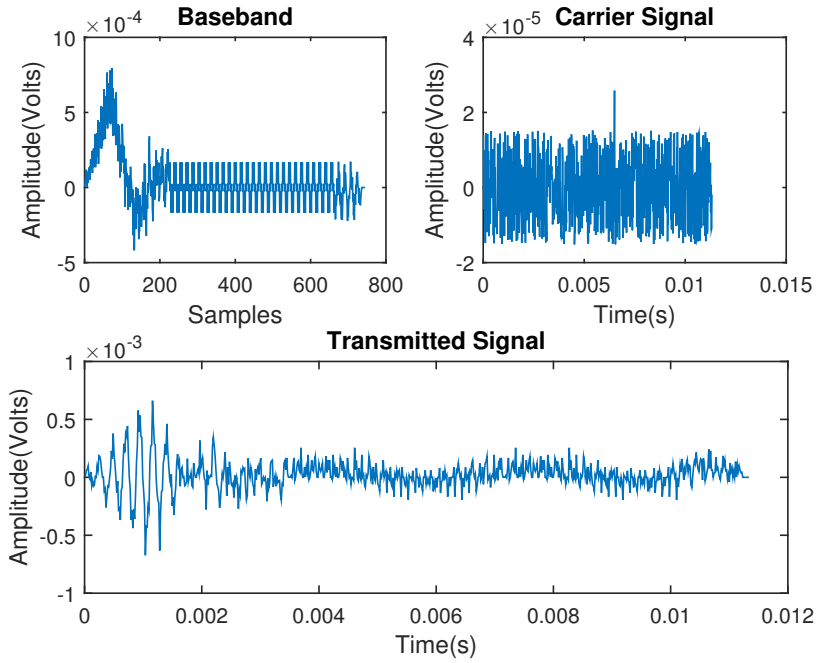

Figure 5.10: *Rounding errors introduced at each stage in the signal chain at the transmitter side due to fixed point representation. It can be observed that the rounding errors gradually increases.*

to the final signal that has to be transmitted. However, the quality of transmission is not affected because the rounding errors are too small to have any effect in the case of BPSK modulation. But if higher modulation schemes are used these errors could increase significantly, affecting the quality of the transmission. From Figure 5.8 it is clear that BPSK transmission is feasible using a 16-bit representation.

6

Results and Discussion

The feasibility of PLC depends on data manipulation in the hardware, as well as on how the received signal is affected by the noise and channel. In this chapter, issues related to hardware and transmission channel are discussed separately based on the data obtained from actual measurements. From the data we draw conclusions on how large impact the hardware as well as the channel have on PLC in vehicles. Also, the implication of the simplification in the measurements and modelling methods is addressed.

6.1 Fixed-Point Hardware

The feasibility of using a fixed-point representation depends on the dynamic range of the fixed-point hardware. In this project we used the 16-bit processor TMS320C5515 to determine the rounding errors for the basic modulation scheme. This experiment was done by implementing mainly the modulator and demodulator for the BPSK scheme, since the rounding errors only affect these blocks. The processing in the remaining blocks of a digital communication system is entirely digital, hence they are not affected by the rounding errors unless measures have been taken to prevent overflow of data between the blocks.

The rounding errors introduced at the transmitter during modulation using BPSK are shown in Figure 5.10. It can be argued that the rounding errors will impact QPSK in a similar fashion since the distance between adjacent constellation points is the same for both BPSK and QPSK in the signal space. This is the deciding factor for the mapping of symbols to bits at the receiver. Although the rounding errors gradually increase, the quality of the transmitted signal is not affected to a level where the final transmitted signal misrepresents the data. However, the SNR of the received signal is reduced significantly due to the poor resolution of the ADC (10 bits). Even so, by using noise shaping techniques we were able to successfully decode the signal.

The obtained results are based only on the RRC pulse-shape used to generate the pulse-train. There are many other pulse-shapes which could be used depending on the application, such as rectangular and raised cosine [22] which may provide better results. Therefore, we can conclude fixed-point processors are feasible for BPSK and QPSK modulation schemes if an RRC pulse shape is used. Apart from the fixed-point representation there are other aspects of the processor that can be of concern, namely memory and

speed. In our case the memory restricted the maximum frame size to 64 bits. This restriction makes the implementation slower since each frame needs to transfer a number of extra bits. A possible change in the algorithms might result in a more memory efficient implementation.

6.2 Channel

The channel model must describe how the output varies for different input frequencies under the influence of noise. This is done in order to know under what conditions and to what extent PLC can be used for transmission of data. We obtained models for the channel and the noise separately using different methods, mostly due to the nature of the data available. The data used for the channel modelling is deterministic whereas in the case of noise the data is completely random.

In order to find the frequency response of the channel we acquired data from both input and output for different wires with varying lengths, gauges and twisting. We used a black-box modelling approach, in particular the ARX-method, to model the channel. The bode plot of the resulting function is shown in Figure 4.6. According to the figure, the channel acts as an low-pass filter with a cut-off frequency of approximately 14 MHz. For modelling the noise, we acquired the data from an actual truck while the engine was running. The variation of loads connected to the power grid was achieved by switching different appliances connected to the power grid of the truck, such as turning indicators, brakes, wiper motors etc. When we estimated the PSD of the acquired data (shown in Figure 4.11), we realised that it is a colored noise. Hence, we modelled an LTI system such that it takes white noise as input and produces colored noise as output. The AR-process was used to estimate the PSD of the noise (as shown in 4.13). The difference equation representing the noise is given by (4.2).

The estimation of both the channel and the noise is obtained from limited data. This means that the data will not cover all the possible circumstances that occur in reality. As a result, the model is an approximation obtained from a few cases and therefore cannot be used for a general description of the actual scenario of the channel found in vehicles. Rather the model partially describes the truck from which we acquired the data. Additionally, the quality of the data is restricted by the oscilloscope's sampling frequency. To be absolutely conclusive, further measurements need to be performed that covers all possible scenarios that could occur. The other issue with the present model is that the parameters are not well defined to represent the actual environment.

In order to study the effects of switching in detail, we conducted simple experiments described in Section 3.2.1. We found that the transfer function changes during switching, reducing the cut-off frequency of the channel. As discussed in Section 3.2.1, the change in transfer function is due to an increase of the capacitance in the channel. The increase in capacitance is directly proportional to the current through the channel, which depends on the loads connected to the wiring harness. This is a very complex problem, since the variations could occur in various stages: 1. Variations in the path of the return current 2. Variation in the loads connected at any given time 3. Variation in the amplitudes and the occurrences of the impulses to name a few. Also, these factors themselves depend on various other factors.

Based upon these results, the implementation of PLC in vehicles is largely a question of how the wiring topology is designed. PLC has been successfully implemented for residential purposes as the situation is different in the case of the residential environment. In case of residential PLC, the return path is more deterministic with 3-wire wiring topology. Again the impulses caused due to switching of loads is predictable unlike in vehicles where it is completely random. Therefore one of the possible changes to ease the implementation of PLC in vehicles is to change the wiring topology.

One possible alternative to reduce the wires other than PLC could be to implement wireless transceivers. As wireless networks the need for wires will not arise, and the current protocols would be obsolete. However, this has issues that relates to spectrum availability, data security and signal interference. The vehicle industry must standardise the frequency spectrum.

7

Conclusion

MANY aspects must be taken into account while implementing PLC in vehicle but one that requires greater attention is the fault tolerance. The impact of a failed transmission in safety-critical systems might have catastrophic consequences, therefore PLC is suitable only for selected applications. Most likely the safety-critical systems should not be used for the first implementation. It might even be so that safety-critical systems never should be implemented using PLC since the noise is of such a rough character. Examples of functions that could be implemented in the first run are the wipers, air conditioning, infotainment etc.

PLC must be proven reliable enough without any errors in order to implement all the vehicle functionality. Proving such reliability is a substantially difficult task since all possible scenarios must be taken into account as well as different vehicle types. Error correction will be of essence to handle faults in the transfer. However, under some circumstances the transient impulses will be so large that entire packages can be considered lost. This makes the possibility of using safety-critical systems doubtful, at least with the current wire topology and electrical system. As discussed earlier, while the obtained results show that fixed-point arithmetic's is possible to use for implementing PLC, there might still be more suitable options available. There is always a trade-off between performance, cost and development time which makes the decision on what hardware to use difficult. When it comes to channel modelling, a better approach would be to describe the channel by using state space models, so that the parameters can capture the real scenario to some extent. In this way it might be possible to address more scenarios through modelling.

Finally, it is neither the hardware nor the background noise that act as constraints. Rather, its the variation of load impedances that are connected to the wiring harness. For this reason we think that the future of PLC in vehicles is that it will remain a concept unless the wiring topology is changed to have deterministic impedance. Additionally, using more complex modulation scheme such as Orthogonal Frequency Division Multiplexing (OFDM) could make PLC a feasible solution because OFDM signals are longer in duration than MC modulation signals in time domain. So even if the load switching occurs which is usually of short duration, the receiver will still be able to recover data. However, implementing OFDM using fixed point DSPs is still a feasibility question. One possible alternative to reduce the wires other than PLC could be to implement wireless transceivers for which the need for wires will not arise, and the current protocols would be obsolete. However, OFDM requires spectrum availability, data security and minimum signal interference which makes it difficult to implement such a system.

Bibliography

[1] R. Hegde, S. Kumar, and K. Gurumurthy, "The impact of network topologies on the performance of the in-vehicle network," in *International Journal of Computer Theory and Engineering, June 2013*, vol. 5, June 2013, pp. 405–409.

[2] S. Tuohy, M. Glavin, C. Hughes, E. Jones, M. Trivedi, and L. Kilmartin, "Intra-vehicle networks: A review," *Intelligent Transportation Systems, IEEE Transactions on*, vol. 16, no. 2, pp. 534–545, April 2015.

[3] FlexRay Consortium. (2006, Nov) *Flexray Communication systems* [Online]. Available: http://tge.cmaisonneuve.qc.ca/barbaud/R%C3%A9f%C3%A9rences%20techniques/Protocoles%20%C3%A0%20tranches%20de%20temps/FlexRay_Electrical_Physical_Layer_Specification_V2.1_Rev.B.pdf. Accessed: 2015-07-06.

[4] Navet, Nicolas and Simonot-Lion, Françoise. (2013, Aug 31) *In-vehicle communication networks-a historical perspective and review* [Online]. Available: https://orbilu.uni.lu/bitstream/10993/5540/1/trends2013.pdf. Accessed: 2015-05-14.

[5] K. H. Johansson, M. Törngren, and L. Nielsen, "Vehicle applications of controller area network," in *Handbook of networked and embedded control systems*. Springer, 2005, pp. 741–765.

[6] L. D'Orazio, F. Visintainer, and M. Darin, "Sensor networks on the car: State of the art and future challenges," in *Design, Automation Test in Europe Conference Exhibition (DATE), 2011*, March 2011, pp. 1–6.

[7] S. A. Tretter, *Communication System Design Using DSP Algorithms: With Laboratory Experiments for the TMS320C6713™ DSK*. Springer, 2008.

[8] M. Antoniali, M. Girotto, and A. Tonello, "In-car power line communications: Advanced transmission techniques," *International Journal of Automotive Technology*, vol. 14, no. 4, pp. 625–632, 2013.

[9] S. Barmada, M. Raugi, M. Tucci, Y. Maryanka, and O. Amrani, "Plc systems for electric vehicles and smart grid applications," in *Power Line Communications and Its Applications (ISPLC), 2013 17th IEEE International Symposium on*, March 2013, pp. 23–28.

[10] T. Rybak and M. Steffka, *Automotive electromagnetic compatibility (EMC)*. Boston, Mass; London: Kluwer Academic, 2003.

[11] N. Taherinejad, R. Rosales, S. Mirabbasi, and L. Lampe, "On the design of impedance matching circuits for vehicular power line communication systems," in *Power Line Communications and Its Applications (ISPLC), 2012 16th IEEE International Symposium on*, March 2012, pp. 322–327.

[12] A. Vallejo-Mora, J. Sánchez-Martínez, F. Cañete, J. Cortes, and L. Diéz, "Characterization and evaluation of in-vehicle power line channels," in *Global Telecommunications Conference (GLOBECOM 2010), 2010 IEEE*, Dec 2010, pp. 1–5.

[13] A. Schiffer, "Statistical channel and noise modeling of vehicular dc-lines for data communication," in *Vehicular Technology Conference Proceedings, 2000. VTC 2000-Spring Tokyo. 2000 IEEE 51st*, vol. 1, 2000, pp. 158–162.

[14] M. Lienard, M. Carrion, V. Degardin, and P. Degauque, "Modeling and analysis of in-vehicle power line communication channels," *Vehicular Technology, IEEE Transactions on*, vol. 57, no. 2, pp. 670–679, March 2008.

[15] H. C. Ferreira, L. Lampe, J. Newbury, and S. G. Theo, *Power Line Communications : Theory and Applications for Narrowband and Broadband Communications over Power Lines.* John Wiley & Sons, 2010.

[16] F. Nouvel and P. Tanguy, "Towards power line communication in vehicle," in *General Assembly and Scientific Symposium, 2011 XXXth URSI*, Aug 2011, pp. 1–4.

[17] R. Yates. (2013, June 2) *Fixed-point arithmetic: An introduction* [Online]. Available: http://www.digitalsignallabs.com/fp.pdf. Accessed: 2015-03-14.

[18] D. Goldberg, "What every computer scientist should know about floating-point arithmetic," *ACM Computing Surveys (CSUR)*, vol. 23, no. 1, pp. 5–48, 1991.

[19] S. W. Smith, *The Scientist and Engineer's Guide to Digital Signal Processing.* San Diego, CA, USA: California Technical Publishing, 1997.

[20] D. Liu, *Next generation SSH2 implementation: securing data in motion.* Syngress, 2011.

[21] N. Alpern, *Eleventh Hour Network+: Exam N10-004 Study Guide.* Syngress, 2010.

[22] J. B. Anderson, *Digital transmission engineering.* John Wiley & Sons, 2006.

[23] K. J. Keesman, *System identification: an introduction.* Springer, 2011.

[24] L. Ljung, *System identification.* Springer, 1998.

[25] S. Miller and D. Childers, *Probability and random processes: With applications to signal processing and communications.* Academic Press, 2012.

[26] M. H. Hayes, *Statistical digital signal processing and modeling.* John Wiley & Sons, 1996.

[27] Texas Instruments. (2013, Oct) *TMS320C5515 Fixed-Point Digital Signal Processor* [Online]. Available: http://www.ti.com.cn/cn/lit/ds/sprs645f/sprs645f.pdf. Accessed: 2015-02-05.

[28] Analog Devices. (2014, May) *AD5686R datasheet* [Online]. Available: http://www.analog.com/media/en/technical-documentation/data-sheets/AD5686R_5685R_5684R.pdf. Accessed: 2015-01-17.

[29] Texas Instruments. *Code Composer Studio (CCS) Integrated Development Environment (IDE)* [Online]. Available: http://www.ti.com/tool/ccstudio#TechnicalDocuments. Accessed: 2015-02-01.

[30] F. Maloberti, *Data converters*. Springer, 2007.

[31] Texas Instruments. (2009, Sep) *TMS320C5515/14/05/04/VC05/VC04 DSP Timer/Watchdog Timer User's Guide* [Online]. Available: http://www.ti.com.cn/cn/lit/ug/sprufo2/sprufo2.pdf. Accessed: 2015-02-12.

[32] Texas Instruments. (2009, Sep) *TMS320C5515/14/05/04/VC05/VC04 DSP Serial Peripheral Interface (SPI) User's Guide* [Online]. Available: http://www.ti.com.cn/cn/lit/ug/sprufo3/sprufo3.pdf. Accessed: 2015-02-12.

[33] Texas Instruments. (2005, Feb) *TMS320C55x DSP CPU Programmer's Reference Supplement* [Online]. Available: http://www.ti.com.cn/cn/lit/ug/spru652g/spru652g.pdf. Accessed: 2015-02-18.

[34] Texas Instruments. (2012, Jan) *TMS320C5515/05/VC05 DSP Successive Approximation Register (SAR) Analog-to-Digital Converter (AC) User's Guide* [Online]. Available: http://www.ti.com.cn/cn/lit/ug/sprufp1c/sprufp1c.pdf. Accessed: 2015-02-16.

[35] J. M. Cioffi. (2007, Jan 7) *Digital Communication: Signal Processing* [Online]. Available: http://web.stanford.edu/group/cioffi/doc/book/chap1.pdf/. Accessed: 2015-03-14.

[36] R. Gonsalves, "Maximum-likelihood receiver for digital data transmission," *Communication Technology, IEEE Transactions on*, vol. 16, no. 3, pp. 392–398.

A

Appendix 1

A.1 Measurement of noise

- **Aim:**
  To measure the noise present in the wires of an actual vehicle under different conditions.
- **Apparatus:**
  1. A digital oscilloscope (TBS 1052B-EDU) with a sampling frequency of 1 Giga samples per second.
  2. A probe whose capacitance is compensated to measure high frequency signals.
  3. Breakout box to measure the signal at different points in the vehicle.
- **Procedure**
  In order to remove the DC from measurement, the coupling in the oscilloscope was switched to AC. The signals were measured at various points in the vehicle such as direction indicators, position lights and break lights under two cases, namely; when the engine was ON and OFF. All the samples were transferred to the computer for further analysis using a USB stick.

A.2 Basic Configuration of TMS320C5515

In order to get the data both out from and into the DSP it is important to configure the peripherals of the device. It is a bit troublesome to obtain the proper information on how to configure the DSP peripherals. There are a large amount of documents apart from the main data sheet available about the DSP. Each peripheral has a dedicated user's guide that describes how it is to be configured. The peripherals we are using is SPI, timer interrupts and ADC.

A.2.1 SPI

To convert the processed data from the DSP into an analog signal the DAC AD5686R is used. The DAC uses SPI for communication, thus the DSP needs to be configured

appropriately for this purpose. There is a user's guide available [31] for the SPI that should be referred. The highest frequency possible is 25 MHz, which is what we are using. Data is shifted out on rising edge and input is captured on falling edge. No interrupts will be enabled.

The DAC needs to be passed a 24-bit message at each transmission. This message starts with a 4-bit command word to tell the DAC what type of operation is being done, in our case this will be that the input register immediately updates the output register after each transfer. The following 4 bits are addressing, the chip itself contains four DACs and the one to be used will be specified here. The final 16 bits are the message itself.

A.2.2 Timer Interrupts

The sampling of the data signal that is to be transmitted is done by using timer interrupts at certain intervals. Whenever an interrupt occurs, a flag is set to indicate that one sample of the signal is to be transmitted over the SPI. Enabling the timer interrupts is not a straightforward process and it is a bit cryptic to get it to work. There are two documents in where to find the proper information; one is the "Timer/Watchdog user's guide" [32] and the other is chapter 5 of "C55x v3.x CPU Reference Guide" [33]. In order to use the interrupts it is necessary to create an interrupt vector pointer table. This table will then point to an interrupt handler that will perform a given task whenever the interrupt is given. The speed in our case is set to 50000000 Hz/ (249 + 1) = 200000 Hz.

A.2.3 ADC

As mentioned before, the ADC is embedded in the DSP itself. It is used to operate at the maximum frequency of 2 MHz. For more information refer to the ADC user's guide in [34].

A.3 List of Hardware

A list of all the hardware used for the implementation and channel measurement follows.

Implementation:

- DSP - TMS32C5515 eZdsp
- DAC - AD5686R
- Connection cables
- Expansion adapter for eZdsp

Channel Measurements:

- Metal Sheets - 1000 x 500 x 1.2 mm

- 4 AWG wire
- 10 AWG wire
- 16 AWG wire
- 20 AWG wire
- 12 volt car battery
- Resistors of various sizes
- Capacitor to block DC voltage
- Arduino Uno
- Solid state relay - SSR-10DD DC/DC

A.4 Oscilloscope Configuration for Channel Measurement

```
Model:DS2302A
SN:DS2D163451774
Manufacturer:RIGOL TECHNOLOGIES
Hardware Ver:2.0
Firmware:00.03.01.00.04

CH1:On
Scale:2.000e+03mV/
Position:1.052e+04mV
Coupling:DC
Invert:Off
Bandwidth Limit:OFF
Probe Ratio:1X
Impedance:50ohm
Unit:V
User Cal:0ps

CH2:On
Scale:5.000e+03mV/
Position:-1.000e+04mV
Coupling:DC
Invert:Off
Bandwidth Limit:OFF
Probe Ratio:1X
Impedance:50ohm
Unit:V
User Cal:0ps

DSO Horizontal System
Delay:Off
```

```
Time Vernier:Off
Time Mode:YT
Time Scale:1.000000e-06s
Delay Time Scale:5.000000e-07s
Time Offset:0.000000e+00s
Delay Time Offset:0.000000e+00s

DSO Acquire System
Acquire Mode:Normal
Memory Depth:70000
Average Num:2
Sampling Rate:1.000e+09
```

A.5 Oscilloscope Configuration for Noise measurement

```
Record Length, 2.500000e+03
Sample Interval, 4.000000e-08
Trigger Point, 1.250000000000e+
Source CH1,  -0.000049760000,
Vertical Units V,  -0.0000497
Vertical Scale, 1.000000e-01
Vertical Offset, 0.000000e+00
Horizontal Units, s  -0.00004
Horizontal Scale, 1.000000e-05,
Pt Fmt Y, -0.000049520000,
Yzero, 0.000000e+00
Probe Atten, 1.000000e+01
Model Number, TBS1052B-EDU
Serial Number, C013400
Firmware Version, FV:v2.52
```

A.6 Miscellaneous

- **Sampling Receiver**: The sampling receiver is a receiver that works by taking samples at regular time intervals. The time interval is equal to the symbol time.
- **Eye Diagram**: The correctness of the sampling instants can be determined easily with the help of an eye diagram. It is obtained by retracing the received signal at regular intervals which takes the shape of an eye, as shown in Figure A.3. The width in the middle of the eye diagram is proportional to the SNR of the received signal. As a consequence, it provides information regarding the correctness of the sampling instant.
- **Signal Constellation**: A signal constellation is a set of M vectors, x_i,*i=0,...,M-1.* The corresponding set of modulated waveforms x_i*i=0,...,M-1* is a signal set [35].

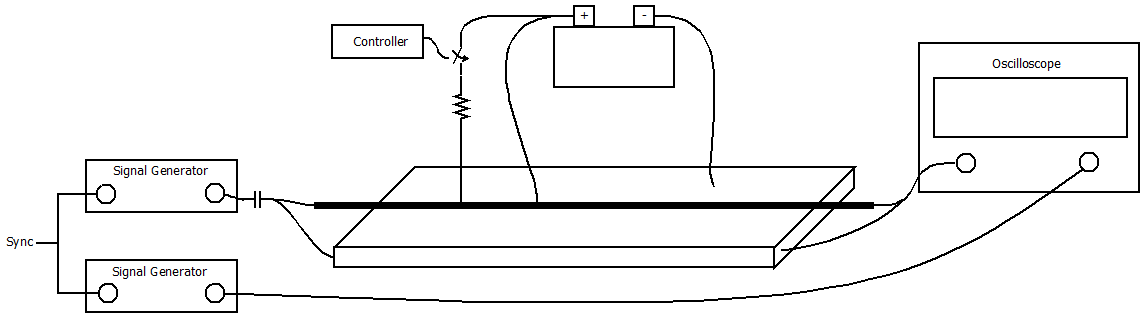

Figure A.1: *Set up used for obtaining the data required for modelling the channel.*

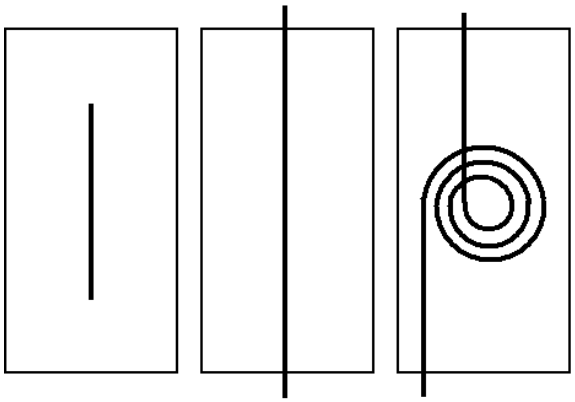

Figure A.2: *The wire configurations: 1 m straight, 2 m straight and 7.25 m curved.*

- **Frequency Masking**: While estimating the PSD, the main lobe masks the side lobes, this is known as frequency masking.
- **Frequency Resolution**: It signifies how well two different peaks can be distinguished in a PSD.
- **Wide sense stationary process**: A stochastic process whose statistical properties such as mean, auto-correlation function depends only on lag alone and is independent of time.
- **Maximum likelihood receiver**: The concept of a maximum likelihood receiver is to estimate the received signal instead of fully recreating it like in an optimum linear receiver. This should be done without the adding of errors [36].
- **Ergodicity of a random process**: A stochastic process is said to be ergodic in mean if the ensemble-average (E(x)) from many realisations can be calculated using the time-average of a single realisation.
- **Peaks and Valleys**: The maximum and minimum points in a PSD are referred to as peaks and valleys.
- **Barker code**: It is an N-bit sequence consisting of 1 and -1 and is used for timing synchronization at the receiver side. The barker sequence has an unique property that is its auto-correlation sequence peaks only when two barker sequences of a given length are perfectly correlated [22].

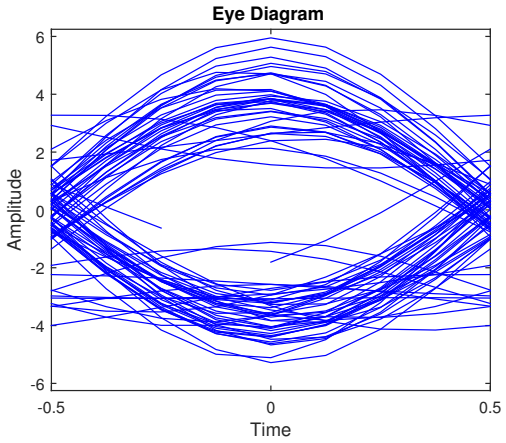

Figure A.3: *Wider opening signifying correct sampling instant and higher SNR.*

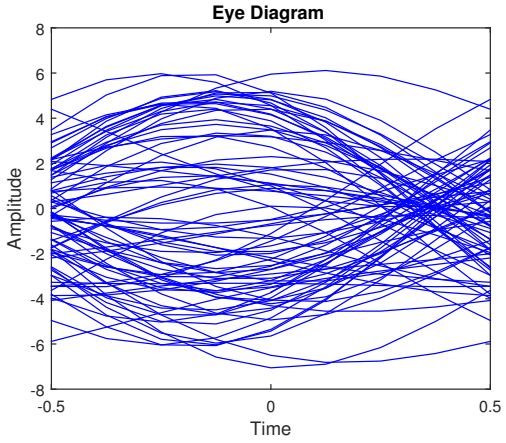

Figure A.4: *Signal with noise when sampled at same instant as Figure A.3.*